Tectonics®

RESEARCH ARTICLE
10.1029/2024TC008748

Key Points:

- Permian development of the western Yukon-Tanana terrane occurred in a supra-subduction setting during closure of the Slide Mountain Ocean
- New U-Pb zircon dates eliminate previous constraints on the "Klondike orogeny" and highlight the effects of Pb loss in metamorphic rocks
- Mid-crustal deformation and metamorphism of the Yukon-Tanana terrane is related to Early Jurassic accretion of the Intermontane terranes

Correspondence to:

M. Colpron,
maurice.colpron@yukon.ca

Citation:

Colpron, M., McClelland, W. C., Piercey, S. J., Kroeger, E. D. L., Crowley, J. L., & Gehrels, G. E. (2025). Revisiting the "Klondike orogeny": Permian to Jurassic development of the Yukon-Tanana terrane, northern Canadian Cordillera. *Tectonics*, *44*, e2024TC008748. https://doi.org/10.1029/2024TC008748

Received 28 NOV 2024
Accepted 28 MAY 2025

Author Contributions:

Conceptualization: Maurice Colpron, William C. McClelland, Stephen J. Piercey
Data curation: Maurice Colpron, William C. McClelland, Stephen J. Piercey
Formal analysis: Maurice Colpron, William C. McClelland, Stephen J. Piercey, Emma D. L. Kroeger, James L. Crowley, George E. Gehrels
Funding acquisition: Maurice Colpron
Investigation: Maurice Colpron, William C. McClelland, Stephen J. Piercey, Emma D. L. Kroeger
Methodology: Maurice Colpron, William C. McClelland, Stephen J. Piercey, Emma D. L. Kroeger, James L. Crowley, George E. Gehrels
Project administration: Maurice Colpron
Resources: Maurice Colpron, William C. McClelland
Supervision: William C. McClelland
Validation: Maurice Colpron, William C. McClelland, Stephen J. Piercey, Emma D. L. Kroeger, James L. Crowley, George E. Gehrels

Revisiting the "Klondike Orogeny": Permian to Jurassic Development of the Yukon-Tanana Terrane, Northern Canadian Cordillera

Maurice Colpron[1], William C. McClelland[2], Stephen J. Piercey[3], Emma D. L. Kroeger[4], James L. Crowley[5], and George E. Gehrels[6]

[1]Yukon Geological Survey, Whitehorse, YT, Canada, [2]Department of Earth and Environmental Sciences, University of Iowa, Iowa City, IA, USA, [3]Department of Earth Sciences, Memorial University of Newfoundland, St. John's, NL, Canada, [4]Clemson University, Clemson, SC, USA, [5]Boise State University, Boise, ID, USA, [6]Department of Geosciences, University of Arizona, Tucson, AZ, USA

Abstract The Permian evolution of the Yukon-Tanana terrane and closure of the Slide Mountain Ocean in the northern Cordillera have been inferred to culminate in the collisional "Klondike orogeny," a northern extension of the Sonoma orogeny of the western USA. The "Klondike orogeny" was thought to be associated with mid-crustal deformation and metamorphism and development of a thick orogenic welt in the late Permian (ca. 260–252 Ma; Lopingian). A review of lithogeochemical data combined with new U-Pb geochronology and Hf isotope data of igneous and detrital zircons from the western Yukon-Tanana terrane supports development of a mid to late Permian (ca. 265–255 Ma; Guadalupian-Lopingian) arc in a supra-subduction zone setting. Arc development was preceded by hyper-extension and emplacement of supra-subduction zone ophiolites (ca. 268–264 Ma). Precise CA-TIMS U-Pb dating of zircon in plutons inferred to constrain the timing of the "Klondike orogeny" show that they are the same age (ca. 260.9 Ma) and that previous dates are too young due to unmitigated Pb loss. A critical review of evidence for regional metamorphism indicates that mid-crustal deformation and metamorphism is related to accretion of the Intermontane terranes in the Early Jurassic. Mica cooling ages show that the western Yukon-Tanana terrane was exhumed to upper crustal level in the Jurassic. Sinistral transpression facilitated development of the Yukon-Tanana terrane and subsequent tectonic activity from mid-Paleozoic to early Mesozoic and probably linked the Permian closure of the Slide Mountain Ocean with intermittent late Paleozoic deformation culminating in the Sonoma orogeny of the U.S. Cordillera.

1. Introduction

The North American Cordillera is an accretionary orogen that was constructed by successive accretion of allochthonous terranes to the western edge of the North American craton mainly in Mesozoic–Cenozoic (Figure 1; e.g., Coney et al., 1980; Monger & Nokleberg, 1996; Monger et al., 1972). The allochthonous terranes are composed of volcanic, plutonic, sedimentary, and metamorphic assemblages that originated as part of microcontinents, magmatic arcs, accretionary complexes, and segments of ocean basins (e.g., Colpron & Nelson, 2021; Nelson et al., 2013; Nokleberg et al., 2000). Stratigraphic, paleomagnetic, faunal and detrital zircon provenance analyses indicate that the terranes have a range of Paleozoic paleogeographic origins with ultimate sources in Baltica, Siberia, northeastern Laurentia and western Laurentia (e.g., Bazard et al., 1995; Colpron & Nelson, 2009, 2011; McClelland et al., 2021; Miller et al., 2011; Soja, 2008).

The Yukon-Tanana terrane is a pericratonic terrane in the northern Cordillera that developed outboard of the western Laurentian margin in mid to late Paleozoic (Mortensen, 1992; Nelson et al., 2006). It consists of successions of metamorphic rocks that record the onset of arc magmatism along western Laurentia in Late Devonian, latest Devonian to Mississippian rifting related to opening of the Slide Mountain back-arc ocean, and development of a Carboniferous island arc built on a rifted fragment of the continental margin (Colpron et al., 2007; Colpron, Nelson, & Murphy, 2006; Kroeger et al., 2023; Mortensen, 1992; Nelson et al., 2006). The last stage of development of the Yukon-Tanana terrane has been related to closure of the Slide Mountain Ocean, recorded in a belt of mid to late Permian (Guadalupian-Lopingian) high-pressure metamorphism (eclogite, blueschist; Erdmer et al., 1998; Petrie et al., 2016), felsic magmatism in parts of the terrane (Mortensen, 1990), and deposition of a Middle to Late Triassic clastic overlap assemblage with sources in both Yukon-Tanana and western Laurentia (e.g., Beranek et al., 2010; Beranek & Mortensen, 2011; Golding et al., 2016).

Visualization: Maurice Colpron, Stephen J. Piercey
Writing – original draft: Maurice Colpron
Writing – review & editing: William C. McClelland, Stephen J. Piercey, Emma D. L. Kroeger, James L. Crowley

Two end-member models have been proposed for the Permian evolution of the Yukon-Tanana terrane. An earlier model proposed closure of the Slide Mountain Ocean through west-dipping subduction beneath the Yukon-Tanana terrane (present-day coordinates; e.g., Colpron et al., 2007; Mortensen, 1992; Nelson et al., 2006). This model accounts for the east to west distribution of Slide Mountain oceanic rocks, high-pressure metamorphic rocks, and felsic magmatism of the Klondike assemblage (ca. 269–254 Ma). Beranek and Mortensen (2011) proposed that final closure of the Slide Mountain Ocean resulted in a late Permian (Lopingian, ca. 260–252 Ma) collisional orogeny, the "Klondike orogeny," associated with greenschist to amphibolite facies regional metamorphism and development of a transposition foliation in rocks of the Yukon-Tanana terrane. This model implied burial and deformation of supracrustal arc rocks to mid-crustal depth shortly after their emplacement in an upper plate setting. The "Klondike orogeny" was postulated to represent a northern extension of the Sonoma orogeny of the western United States (e.g., Beranek & Mortensen, 2011; Dickinson, 2004; Miller et al., 1992).

Alternative models proposed by Parsons et al. (2019) and van Staal et al. (2018) considered the occurrence of high-pressure metamorphic rocks in metasedimentary rocks of the Yukon-Tanana terrane and apparently coeval mid-crustal deformation and metamorphism of the terrane during the Permian "Klondike orogeny" to suggest a lower plate position for the terrane. These authors documented development of middle Permian (ca. 268–264 Ma; Guadalupian) supra-subduction zone ophiolites in rocks previously assigned to the Slide Mountain terrane and suggested burial and deformation of Yukon-Tanana along an east-dipping subduction zone beneath the Slide Mountain Ocean. Van Staal et al. (2018) considered multiple scenarios, some with west-dipping subduction and amalgamation of a composite Yukon-Tanana terrane. In these alternative models, the "Klondike orogeny" records collision of the Yukon-Tanana terrane with an intra-oceanic arc, the Klondike magmatism results from non-arc processes, and closure of the Slide Mountain Ocean occurred later in the Jurassic (Parsons et al., 2019; van Staal et al., 2018). In all proposed models, the nature and timing of the "Klondike orogeny" are factors that constrain interpretations.

In this contribution we review the evidence for Lopingian deformation and metamorphism and provide new U-Pb zircon dates and Hf isotope data for detrital and igneous zircons from Permian rocks in the western Yukon-Tanana terrane. We specifically evaluate the idea that parts of the Yukon-Tanana terrane were deformed and metamorphosed at mid-crustal levels in a thick orogen in the Lopingian. We also review the geochemistry and geological setting of Guadalupian–Lopingian igneous rocks in the western Yukon-Tanana terrane, including ophiolitic assemblages previously assigned to the Slide Mountain terrane, and propose revised correlations for these rocks. Our U-Pb results show that Pb loss can be significant in metamorphic rocks of the Yukon-Tanana terrane, leading to misinterpretation of geological events. We caution that careful analysis combining laser ablation inductively coupled mass spectrometry (LA-ICPMS) and high-precision, chemical abrasion thermal ionization mass spectrometry (CA-TIMS) may be required to resolve the timing of geological events in metamorphic terranes. Our analysis of available metamorphic data combined with the new geochronology results shows that there is no substantial evidence for Lopingian mid-crustal deformation and metamorphism in the western Yukon-Tanana terrane, but rather that amphibolite facies metamorphism is an Early Jurassic event related to accretion of the Intermontane terranes and onset of development of the northern Cordilleran orogen (Colpron et al., 2015, 2022).

2. Yukon-Tanana and Related Terranes

The Yukon-Tanana terrane comprises successions of Upper Devonian to Permian metasedimentary and metaigneous rocks that constitute the older components of the Intermontane terranes in Yukon and adjacent parts of east-central Alaska and northern British Columbia (Figure 1). Devonian metaigneous and associated metasedimentary rocks in southeastern Alaska have also been correlated with the Yukon-Tanana terrane (Gehrels et al., 1990, 1992) but recent studies show that they have distinct pre-Carboniferous records compared to the Yukon-Tanana terrane in Yukon (Kroeger et al., 2023; Pecha et al., 2016). The Paleozoic rocks of southeastern Alaska were originally assigned to the Tracy Arm terrane (Coney et al., 1980; Jones et al., 1983) and Kroeger et al. (2023) proposed reverting to this name to highlight these differences (Figure 1). The extent of the Tracy Arm terrane to the north in northwestern British Columbia and its contact relationship with the Yukon-Tanana terrane of Yukon remain enigmatic. Rocks in northwestern British Columbia and adjacent southwestern Yukon are currently assigned to the Yukon-Tanana terrane (Figure 1) but were previously considered part of the Nisling terrane (Currie & Parrish, 1993; Wheeler et al., 1991) and may be related to the Tracy Arm terrane.

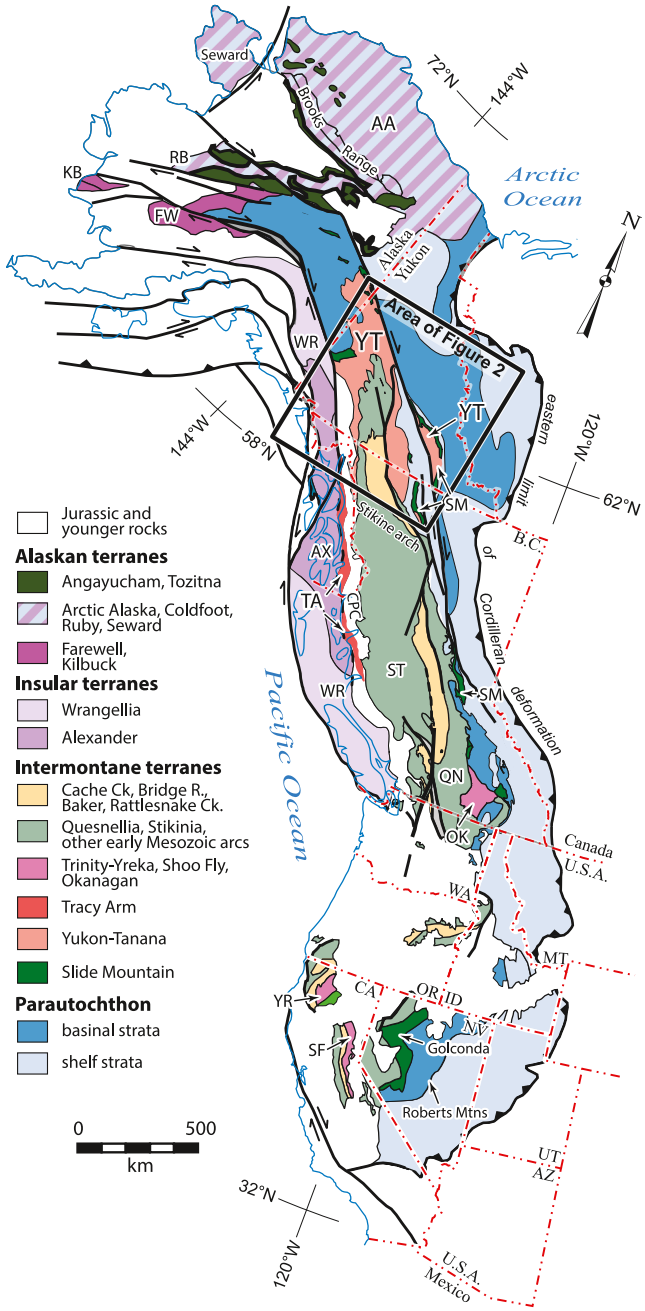

Figure 1. Paleozoic to early Mesozoic terranes of the North American Cordillera. Modified after Kroeger et al. (2023). Location for Figure 2 shown by black box. Abbreviations: AA, Arctic Alaska; AX, Alexander; KB, Kilbuck; OK, Okanagan; QN, Quesnellia; RB, Ruby; RT, Richardson trough; SF, Shoo Fly complex; SM, Slide Mountain; ST, Stikinia; TA, Tracy Arm; WR, Wrangellia; YR, Yreka and Trinity; YSB, Yukon Stable Block; YT, Yukon-Tanana. Other abbreviations: B.C., British Columbia; CA, California; NV, Nevada; OR, Oregon; U.S.A., United States of America.

In Yukon, the Yukon-Tanana terrane lies west of Upper Devonian to lower Permian (Cisuralian) pelagic metasedimentary rocks and oceanic metaigneous rocks of the Slide Mountain terrane (Figure 2). To the west, the Yukon-Tanana terrane is locally intruded by Late Triassic primitive arc plutons and is inferred to form the basement to volcanic arc successions of Stikinia in southern Yukon (Colpron et al., 2022). Exposures of the Yukon-Tanana and Slide Mountain terranes in Yukon were dissected into two main belts after dextral offset of 430–490 km occurred along the Tintina fault in Cenozoic (Figure 2; Gabrielse, 1985; Gabrielse et al., 2006; Roddick, 1967).

The Yukon-Tanana terrane in Yukon comprises three unconformity-bounded volcano-sedimentary successions—the Finlayson, Klinkit and Klondike assemblages—that were deposited on a metasedimentary basement sequence—the Snowcap assemblage—interpreted as a rifted fragment of the western Laurentian continental margin (Figure 3; Colpron, Nelson, & Murphy, 2006; Piercey & Colpron, 2009). The onset of arc magmatism in the Late Devonian was accompanied by rifting and opening of the Slide Mountain back-arc ocean in the latest Devonian to Early Mississippian (Colpron et al., 2007; Creaser et al., 1999; Mortensen, 1992; Nelson et al., 2006). Late Devonian magmatism is recorded both in strata of the western Laurentian continental margin and in the Yukon-Tanana terrane, but younger Carboniferous to Permian magmatism is unique to the terrane, suggesting that the arc migrated away from the continental margin after opening of the Slide Mountain back-arc ocean (Cobbett et al., 2021; Dusel-Bacon et al., 2006, 2017; Nelson et al., 2006). Regional Late Devonian extension along the continental margin is recorded in coarse clastic deposits, local alkaline volcanism, syn-sedimentary faulting, and development of a sub-Frasnian unconformity in the Earn Group of the northern Canadian Cordillera (Cobbett et al., 2021; Gordey et al., 1987).

The main phases of west-facing arc and back-arc development in the Yukon-Tanana terrane are recorded by volcanic and sedimentary rocks of the Upper Devonian to Lower Mississippian Finlayson assemblage and Middle Mississippian to Cisuralian Klinkit assemblage (Colpron, Nelson, & Murphy, 2006; Piercey et al., 2006). This study focuses on the Guadalupian–Lopingian phase of magmatism and sedimentation in the western Yukon-Tanana terrane (Klondike assemblage). More extensive description of the Snowcap, Finlayson and Klinkit assemblages and their regional relationships are presented in Colpron, Nelson, and Murphy (2006), Piercey and Colpron (2009) and Kroeger et al. (2023).

The Guadalupian–Lopingian Klondike assemblage comprises metavolcanic rocks and associated plutons that have been interpreted to record arc magmatism related to closure of the Slide Mountain back-arc ocean (Colpron et al., 2007; Mortensen, 1990, 1992; Nelson et al., 2006). Alternative interpretations have been proposed for the Permian Klondike magmatism (orogenic collapse, extension-related, and/or slab break-off; Parsons et al., 2019; van Staal et al., 2018; Zagorevski & van Staal, 2021). Rocks of the Klondike assemblage are primarily preserved in the Klondike and Dawson Range regions of western Yukon, south of Dawson, and adjacent east-central Alaska, where both metavolcanic (Klondike Schist) and metaplutonic rocks (Sulphur Creek suite) are documented (Figures 2–4). The Klondike Schist (ca. 269–254 Ma) is composed mainly of felsic metavolcanic schist, locally with quartz augen, minor chloritic schist, and micaceous quartzite (Mortensen, 1990, 1996). Primary volcanic and sedimentary textures are locally preserved in the Klondike Schist (Colpron & Ryan, 2010; Ryan et al., 2021). It is locally intruded by variably foliated K-feldspar augen granite and quartz monzonite of the Sulphur Creek plutonic suite (ca. 265–255 Ma). Small-volume intrusions of Permian (ca. 265–257 Ma) metaigneous rocks also occur to the south in Yukon-Tanana

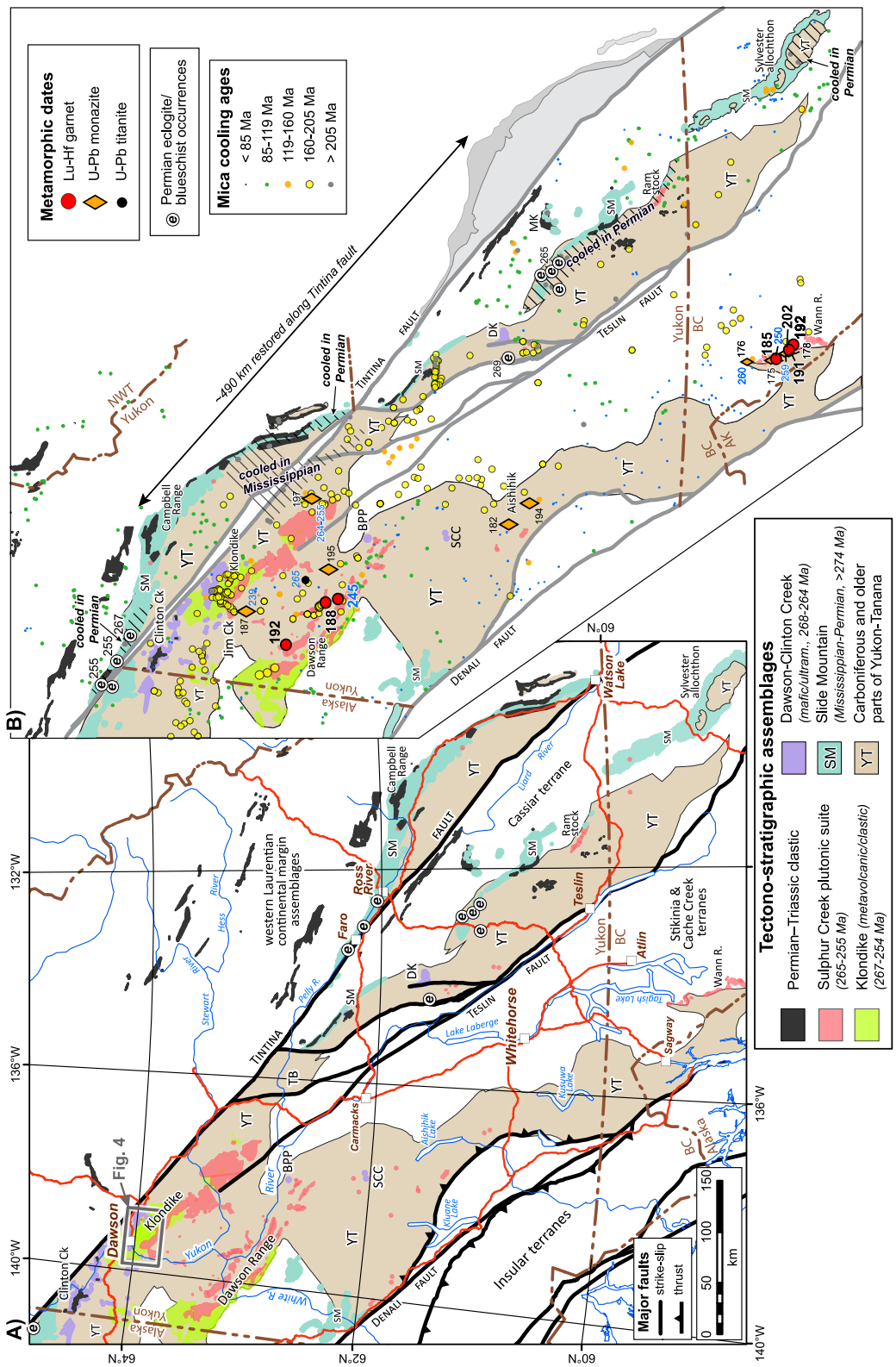

Figure 2. (a) Distribution of Permian tectonostratigraphic assemblages of the Yukon-Tanana and Slide Mountain terranes, and of Triassic overlap assemblages in Yukon and adjacent parts of Alaska and British Columbia. Permian–Triassic geological units were extracted from Yukon Geological Survey (2024), Wilson et al. (2015), and Cui et al. (2017). Gray box south of Dawson indicates the location of the Klondike region shown in Figure 4. (b) Distribution of Permian–Triassic assemblages after restoration of ~490 km of dextral displacement along the Tintina fault. The locations of dated minerals that constrain timing of metamorphism and mica cooling ages are shown. Metamorphic ages are from sources compiled in Table 1. Mica cooling ages are extracted from Yukon Geological Survey (2023) for Yukon, Han et al. (2020) for British Columbia, and Dusel-Bacon et al. (2002) for eastern Alaska. Hatched areas indicate regions of the Yukon-Tanana terrane that were exhumed in the Paleozoic. Abbreviations for localities mentioned in the text: BPP, Buffalo Pitts peridotite; DK, Dunite klippen; MK, McNeil klippe; SCC, Schist Creek complex; TB, Tatlmain batholith.

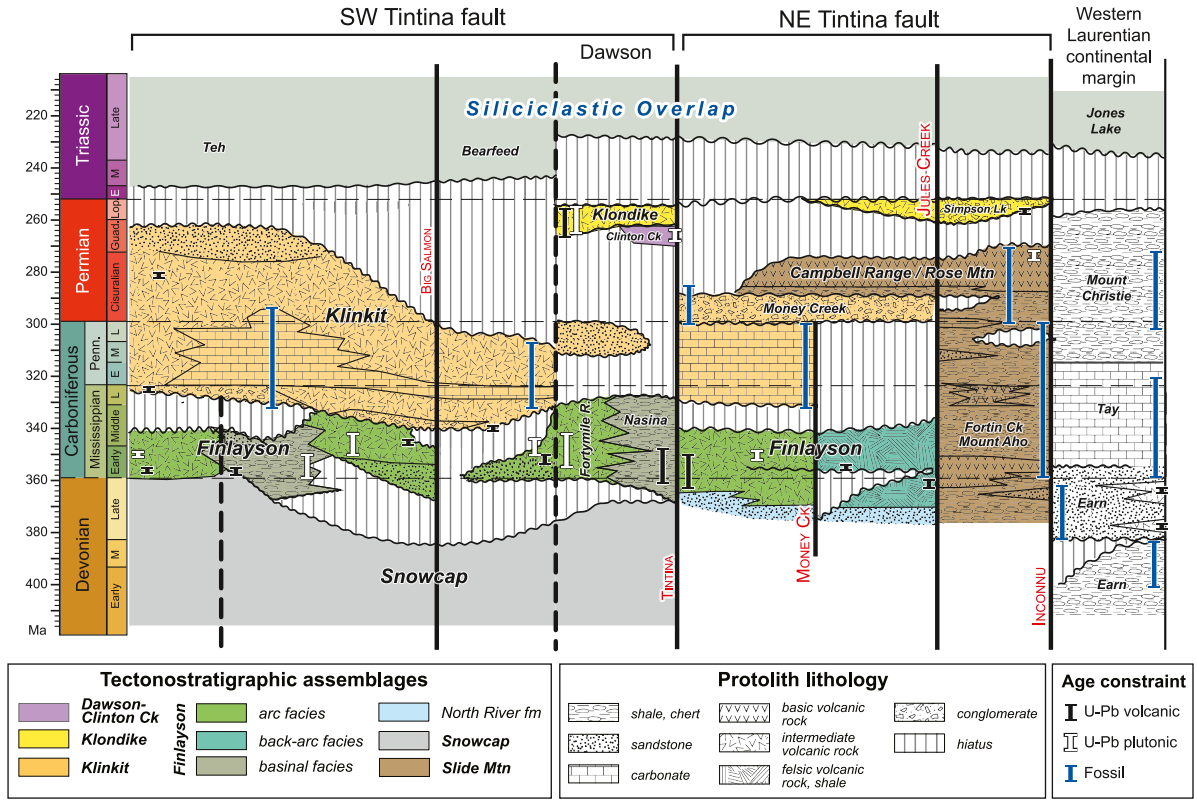

Figure 3. Regional relationships of Paleozoic tectonostratigraphic assemblages in the Yukon-Tanana terrane and coeval successions in the Slide Mountain terrane and western Laurentian continental margin (modified after Kroeger et al. (2023)). Select local stratigraphic names mentioned in the text are indicated. Independent age constraints for local units are indicated by vertical bars. Major faults dividing the terrane are shown by heavy, vertical black lines with red labels; dashed lines indicate inferred faults. Timescale generated with TSCreator (https://timescalecreator.org).

and Slide Mountain terranes and may be related to the Sulphur Creek suite of western Yukon, or represent distinct, coeval magmatism (e.g., Ram and Wann River stocks, Figure 2).

The Slide Mountain terrane comprises: (a) a lower unit of predominantly phyllite, argillite and chert with minor felsic and mafic metavolcanic rocks, arkosic grit, conglomerate and quartzite, and rare limestone (Fortin Creek Group and Mount Aho formation, Mississippian to lower Cisuralian); and (b) an upper unit of basalt with intercalated red and green chert and argillite (Rose Mountain and Campbell Range formations, Cisuralian, Figure 3; Murphy et al., 2006; Pigage, 2004). Diabase, leucogabbro and variably serpentinized ultramafic rocks are spatially associated with basalt of the Campbell Range formation and occur locally in the underlying Fortin Creek Group. Leucogabbro bodies in the Campbell Range formation are dated ca. 274 Ma and represent the youngest magmatism in the Slide Mountain terrane (Murphy et al., 2006). Basalts of the Campbell Range formation occur mainly northeast of the fault that juxtaposes older parts of Yukon-Tanana and Slide Mountain terranes (Vangorda–Jules Creek fault; Figure 3), but local basalt exposures southwest of the fault apparently represent an overlap onto the Yukon-Tanana terrane (Colpron et al., 2007; Murphy et al., 2006; Piercey et al., 2012). Strike-slip displacement along the Vangorda–Jules Creek fault is inferred to have occurred in the Cisuralian and later reactivated in the Mesozoic (Murphy et al., 2006; Piercey et al., 2012). Basalt in the Fortin Creek Group and Campbell Range formation generally have mid-ocean ridge (MORB) and back-arc basin (BABB)-type geochemical signatures and juvenile isotopes (εNd_t = +6 to +9). However, exposures of the Campbell Range formation that overlap the Yukon-Tanana terrane have the geochemical character of ocean-island (OIB) and enriched-mid ocean ridge basalt (E-MORB) and less juvenile isotopic values (εNd_t = +2 to +6; Piercey et al., 2006, 2012).

Another belt of ophiolitic rocks structurally imbricated within the western Yukon-Tanana terrane was previously correlated with the Slide Mountain terrane (e.g., Colpron et al., 2016; Gordey & Makepeace, 2001; Mortensen, 1992). The main exposures of ultramafic rocks and greenstone within this ophiolitic belt occur near Dawson

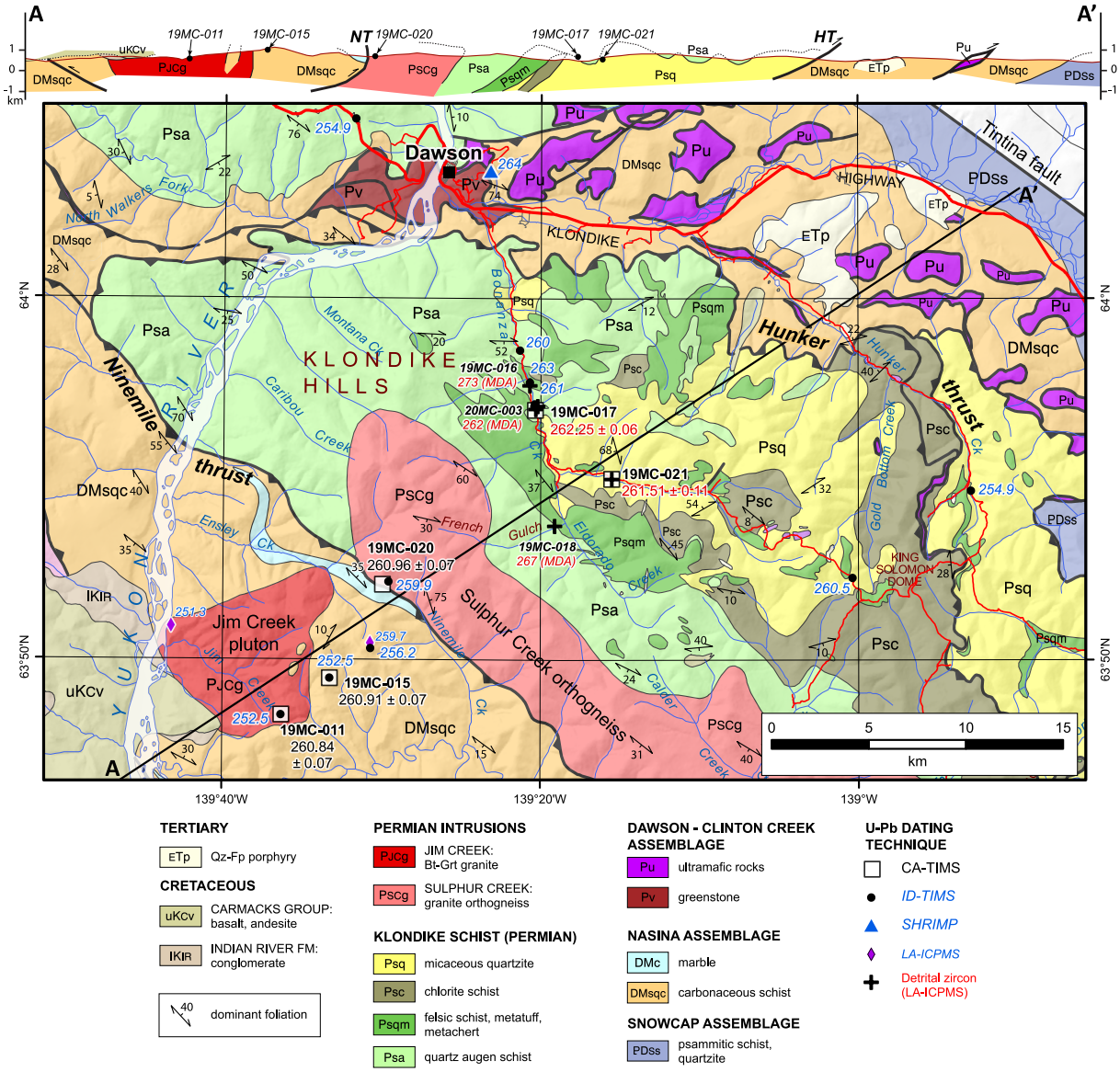

Figure 4. Geological map of the Klondike region, western Yukon. Modified after Mortensen (1996). The location of samples dated by U-Pb zircon are symbolized by dating technique with ages in Ma. Sample numbers are indicated for data presented in this study (Table 2). Igneous ages from this study are shown in black, while red font indicate detrital zircon maximum depositional ages (MDA); all other ages shown in blue are from the Yukon Geological Survey (2023) compilation. Errors (2σ) are shown for samples dated by CA-TIMS in this study (Table 2; Appendix C in Colpron et al. (2025)). Cross-section A-A′ is shown at the top with approximate position of samples dated by CA-TIMS in this study. HT, Hunker thrust; NT, Ninemile thrust.

and at Clinton Creek in western Yukon, inboard of the main belt of Slide Mountain terrane after restoration of Cenozoic displacement along the Tintina fault (Figure 2b). These ultramafic–greenstone complexes were assigned to the Dawson–Clinton Creek assemblage by Mortensen (1996) and we follow this usage here. Recent data from the Dawson–Clinton Creek assemblage warrant subdivision from the Slide Mountain terrane. Gabbro from the Dawson–Clinton Creek complexes yielded U-Pb zircon dates ca. 265–264 Ma and have tholeiitic to calc-alkalic geochemical compositions typical of arc-related magmas (van Staal et al., 2018) that are younger and distinct from the main belt of Slide Mountain terrane in Yukon (Piercey et al., 2006, 2012). These two belts of Permian ophiolitic complexes also extend into eastern Alaska where they are all assigned to the Seventymile terrane but show similar distinction in structural and geochemical characters as the Slide Mountain (Campbell Range formation) and Dawson–Clinton Creek assemblages in Yukon (e.g., Dusel-Bacon & Cooper, 1999; Dusel-Bacon et al., 2006; Dusel-Bacon & Mortensen, 2023, 2024; Figure 2).

Other greenstone and ultramafic complexes associated with the Yukon-Tanana terrane and formerly assigned to the Slide Mountain terrane may also be correlative with the Dawson–Clinton Creek assemblage of western Yukon (Figure 2). These include rocks of the Dunite klippe that have primitive island-arc tholeiite (IAT) geochemical signatures, primitive isotopes ($\varepsilon Nd_t = +7$ to $+9$), and U-Pb zircon dates ca. 268–265 Ma (Parsons et al., 2019). Further, other smaller occurrences of greenstone and gabbro with U-Pb zircon dates of 268–260 Ma and calc-alkalic geochemical signatures may also be correlative with the Dawson–Clinton Creek and/or Dunite assemblages (Colpron et al., 2005; Colpron, Mortensen, et al., 2006; Parsons et al., 2019). The ultramafic–greenstone complexes of the Dawson–Clinton Creek and Dunite assemblages have been interpreted as supra-subduction zone ophiolites that formed in extensional settings (Parsons et al., 2019; van Staal et al., 2018). These authors proposed that ultramafic-greenstone complexes of the Dawson–Clinton Creek and Dunite assemblages should be considered distinct terranes from the Slide Mountain terrane. Parsons et al. (2019) proposed the name of Dunite Peak terrane, while van Staal et al. (2018) suggested retaining the name of Slide Mountain for ophiolitic rocks of the Dawson–Clinton Creek belt and assigning oceanic rocks east of the Yukon-Tanana terrane to the Angayucham terrane. In this paper, we focus specifically on the Dawson–Clinton Creek assemblage and its relations to Permian magmatism of the Klondike assemblage in western Yukon. We follow the nomenclature of Mortensen (1996) for the Dawson–Clinton Creek assemblage, as it has precedence over the more recent studies, and we retain the original name of Slide Mountain terrane for the easternmost belt of oceanic rocks to avoid confusion (Monger et al., 1991).

Small ultramafic bodies also occur farther inboard within the Yukon-Tanana terrane (Buffalo Pitts peridotite [BPP] and Schist Creek complex [SCC] on Figure 2). These have been interpreted as orogenic peridotite emplaced during extension of the Yukon-Tanana terrane ca. 267–262 Ma (Johnston et al., 2007; Ryan et al., 2021).

A narrow belt of Permian (ca. 271–265 Ma) eclogite and blueschist marks the eastern edge of the Yukon-Tanana terrane from eastern Alaska to southern Yukon (Figure 2; Erdmer et al., 1998). Mafic eclogite pods are interleaved with quartzo-feldspathic schist, share deformation fabrics with the host rock, and have pre-metamorphic contacts that are inferred to be intrusive (Erdmer et al., 1998; Gilotti et al., 2017). The eclogite protolith is Late Devonian and has within-plate to normal MORB trace element signatures and primitive isotopic composition (Creaser et al., 1999; Petrie et al., 2016). The host rocks were also deformed and metamorphosed at eclogite facies; they are inferred to form part of the Snowcap metasedimentary assemblage and Carboniferous arc plutons of the Yukon-Tanana terrane (Gilotti et al., 2017; Petrie et al., 2015). The eclogite-facies rocks were exhumed rapidly after metamorphism in Guadalupian–Lopingian (Erdmer et al., 1998; Fallas et al., 1998).

Clastic sedimentary rocks of the Guadalupian to Triassic(?) Simpson Lake Group unconformably overlap the Slide Mountain terrane northeast of the Tintina fault (Figures 2 and 3; Murphy et al., 2006). The Simpson Lake Group is composed of polymictic, cobble to boulder conglomerate and breccia, sandstone, siltstone and shale. Clasts in the conglomerate are mostly locally derived and include foliated chert and carbonaceous phyllite, basalt, ultramafic rocks, felsic and intermediate volcanic rocks of arc affinity, limestone, quartzite, blueschist and eclogite derived from the Slide Mountain and Yukon-Tanana terranes (Mortensen et al., 1997; Murphy et al., 2006). Occurrences of the Simpson Lake Group are localized near the Yukon-Tanana—Slide Mountain boundary, the Vangorda–Jules Creek fault. Foreland, forearc or strike-slip basin depositional settings have been proposed for the Simpson Lake Group (see Murphy et al., 2006).

Fine-grained Triassic siliciclastic rocks unconformably overlie the western Laurentian margin, Slide Mountain and Yukon-Tanana terranes in southern Yukon (Figure 2). The Triassic rocks are characterized across the region by similar lithological assemblages of shale, calcareous siltstone and fine-grained sandstone with common ripple cross-laminations and burrows indicative of deposition on a shallow, wave-influenced shelf (Gordey, 2013; Gordey & Anderson, 1993; Murphy et al., 2006). The Triassic strata range mostly from Ladinian to Rhaetian (Middle to Upper Triassic), with local older Olenekian (Lower Triassic) strata in easternmost exposures on the Laurentian margin (Orchard, 2006). Limestone forms prominent mappable units mainly in Carnian to Norian strata. Coarse-grained conglomeratic facies occur locally on the Slide Mountain and Yukon-Tanana terranes. The Triassic strata were considered a possible overlap succession based on similar lithology and presence of westerly-derived detrital zircon and mica (Beranek & Mortensen, 2011; Gabrielse, 1991; Nelson et al., 2006). Late Triassic conodont fauna from strata overlying the Yukon-Tanana, Slide Mountain and Cassiar terranes (the latter is a displaced fragment of the Paleozoic continental margin southwest of Tintina fault; Figures 1 and 2) suggests deposition in warm waters at lower latitude (Orchard, 2006).

The Yukon-Tanana terrane was intruded by Late Triassic and younger plutons and affected by multiple episodes of Jurassic–Cretaceous deformation and metamorphism (e.g., Berman et al., 2007; Staples et al., 2014). Late Triassic plutons in western Yukon are the inferred roots to Stikinia and indicate that Yukon-Tanana was the local basement to Late Triassic Stikinia (Colpron et al., 2022). Early Jurassic plutons were emplaced at mid-crustal levels during regional deformation and metamorphism of the Yukon-Tanana terrane, in the early stages of collision between the Intermontane terranes and the western North American margin (e.g., Colpron et al., 2015, 2022; Johnston & Erdmer, 1995; Johnston et al., 1996; Kovacs et al., 2020). Imbrications of the Intermontane terranes with the North American margin probably began in the Early Jurassic (ca. 189–185 Ma; e.g., Nixon et al., 2020) and major faults in Yukon are intruded by Early Cretaceous (ca. 105 Ma) plutons (e.g., Pigage, 2004; Yukon Geological Survey, 2024).

Much of the Yukon-Tanana terrane was exhumed in the Early to Middle Jurassic (ca. 205–160 Ma; Figure 2b), within 10–20 m.y. after burial to mid-crustal levels (Colpron et al., 2015, 2022). Despite the generally pervasive Mesozoic overprint of the Yukon-Tanana terrane, parts of the terrane escaped regional deformation and metamorphism, and were exhumed in the Paleozoic (Figure 2b). This includes large parts of the Permian high-pressure metamorphic belt along the eastern edge of the Yukon-Tanana terrane.

2.1. Geology of the Klondike Region

The Klondike region, south of Dawson, Yukon, is primarily underlain by rocks of the Yukon-Tanana terrane imbricated with greenstone–ultramafic rocks of the Dawson–Clinton Creek assemblage along a series of northeast-verging thrust faults (Figure 4; Gordey & Ryan, 2005; MacKenzie et al., 2008a; Mortensen, 1988a, 1996). In this region, the Yukon-Tanana terrane comprises mainly carbonaceous metasedimentary rocks of the Nasina assemblage (part of the regional Finlayson assemblage) and metavolcanic and metasedimentary rocks of the Klondike Schist. The Nasina assemblage consists of fine-grained, carbonaceous schist and phyllite, micaceous quartzite, marble, and rare chlorite schist (Figure 5a; Mortensen, 1988a, 1988b, 1996). West of Dawson, isolated occurrences of felsic schist (metavolcanic and/or metaplutonic) in carbonaceous phyllite of the Nasina assemblage have U-Pb zircon dates of ca. 361–348 Ma (Dusel-Bacon et al., 2006; Dusel-Bacon & Mortensen, 2023, 2024). In the Klondike region, rocks of the Nasina assemblage occur in the footwall of the Hunker thrust to the north, and southwest of the Ninemile thrust (Figure 4).

The Klondike Schist occupies the structural panel between the Ninemile and Hunker thrusts and comprises four map units exposed on the flanks of a structural dome (Figure 4; Mortensen, 1996). Quartz augen schist and gritty quartzite (Psa) at higher structural levels, in the footwall of the Ninemile thrust, are intercalated with and grade eastward into fine-grained quartz-feldspar-muscovite schist and micaceous quartzite (Psqm), and into bands of chlorite schist (Psc) and micaceous quartzite (Psq) at lower structural levels (Figure 4). Unit Psa is inferred to represent a subvolcanic sill complex to felsic metavolcanic rocks of Psqm (Mortensen, 1996). Unit Psa appears gradational into medium to coarse-grained, foliated quartz monzonite to granite, locally with K-feldspar augens, of the Sulphur Creek orthogneiss (Figure 5b). Felsic metavolcanic rocks and quartz augen schist of the Klondike Schist in this region yielded U-Pb zircon dates of 263–253 Ma, while foliated quartz monzonite and granite of the Sulphur Creek orthogneiss has U-Pb zircon dates of 262–260 Ma (Figure 4; Dusel-Bacon & Mortensen, 2023, 2024; Mortensen, 1990). Southwest of the Ninemile thrust, carbonaceous schist of the Nasina assemblage is intruded by two-mica (±garnet) granite of the Jim Creek pluton and related dikes that yielded U-Pb zircon dates ca. 260–252 Ma (Figures 4 and 5c; Beranek & Mortensen, 2011).

Greenstone–ultramafic rocks of the Dawson–Clinton Creek assemblage occur mainly in the footwall of the Hunker thrust in this region (Figure 4). Greenstone and variably serpentinized harzburgite are structurally intercalated with carbonaceous phyllite of the Nasina assemblage. A leucogabbro intruding the ultramafic rocks near Dawson yielded a U-Pb zircon date of 264 ± 4 Ma (van Staal et al., 2018).

Rocks of the Yukon-Tanana terrane in the Klondike region are pervasively foliated and recrystallized, with at least two generations of isoclinal folds (F_1, F_2) superposed by F_3 folds that are open, moderately inclined to recumbent, with local development of spaced and facoidal cleavages (Gordey & Ryan, 2005; MacKenzie & Craw, 2012; MacKenzie et al., 2007, 2008a, 2008b). Ductile fabrics generally increase with proximity to the Hunker and Ninemile thrusts. MacKenzie et al. (2008a) suggested that northeast-directed thrust imbrication was associated with D_3 structures developed in the Jurassic. The Ninemile thrust, which bounds the Klondike Schist and Sulphur Creek orthogneiss to the southwest (Figure 4), has variably been interpreted as northeast-dipping and

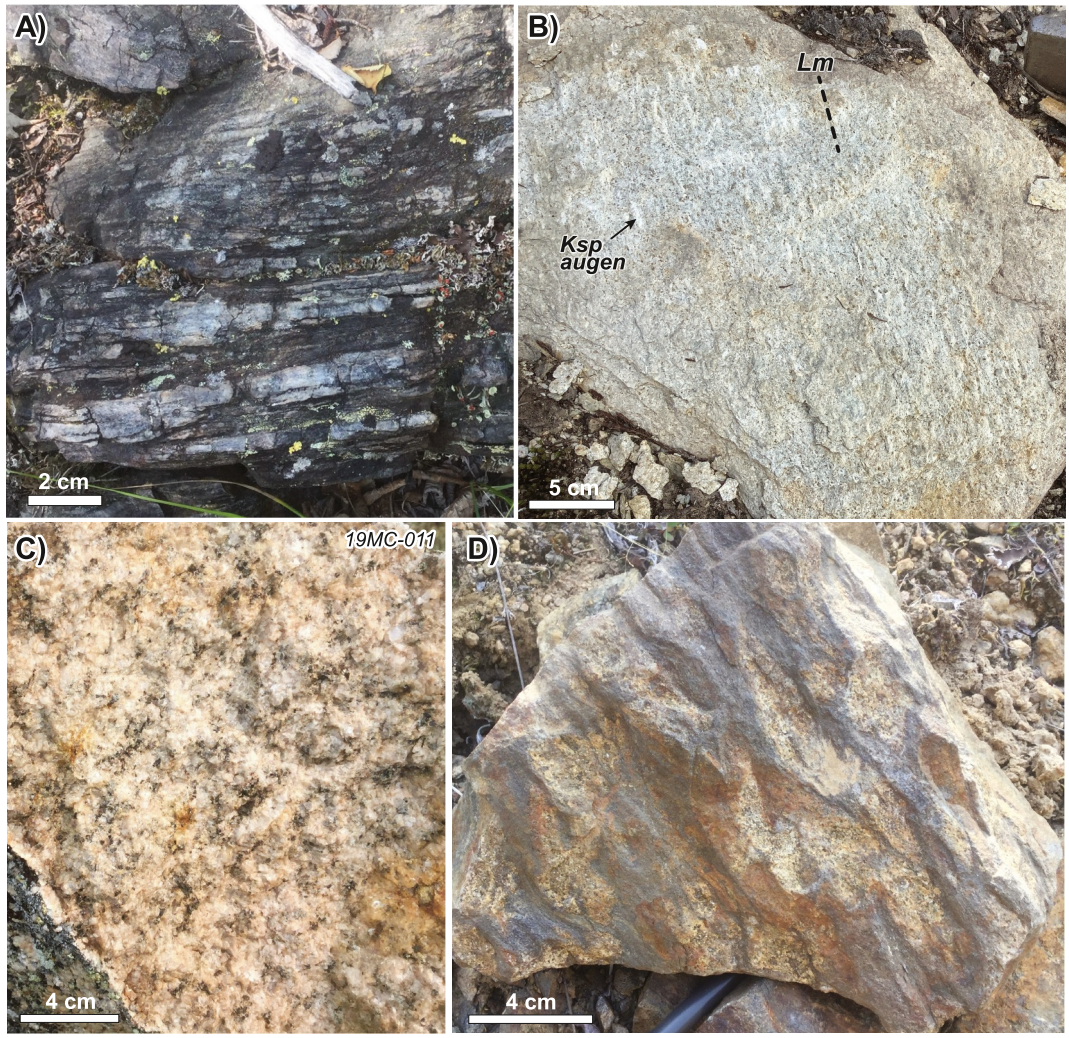

Figure 5. (a) Strongly foliated carbonaceous schist and quartzite of the Nasina assemblage at the headwater of Ensley Creek. (b) Lineated, K-feldspar augen granite, Sulphur Creek orthogneiss near the Ninemile thrust. (c) Coarse-grained two-mica granite from the Jim Creek pluton, locality 19MC-011. (d) Granite apophyses deformed with host schist along the eastern margin of the Jim Creek pluton.

marking the base of a klippe of Klondike assemblage rocks (e.g., Dusel-Bacon & Mortensen, 2023, 2024; Gordey & Ryan, 2005; Mortensen, 1996) or a southwest-dipping fault, locally overturned and juxtaposing rocks of the Nasina assemblage over the Klondike assemblage to the northeast (MacKenzie & Craw, 2012). We favor this latter interpretation in the cross-section on Figure 4 because ductile fabric in the region is dominantly southwest-dipping with exception to exposures at the headwater of Ninemile Creek.

The relationships surrounding the Jim Creek pluton in the hanging wall of the Ninemile thrust are critical to interpretation of the "Klondike orogeny" (Figure 4). Beranek and Mortensen (2011, p. 7) described the Jim Creek pluton and associated dikes as massive and undeformed with sharp contacts cutting the foliation in the Nasina schist (Figure 5c). A strongly foliated quartz monzonite sill intruded in the Nasina schist contains the same deformation fabric as the schist and yielded U-Pb zircon dates of ca. 260–256 Ma (Beranek & Mortensen, 2011). Our observations, however, are that the contacts of the Jim Creek pluton are locally deformed along with the wall rock (Figure 5d).

3. Constraints on Structural and Metamorphic Evolution

The concept that the main penetrative ductile fabric in the Yukon-Tanana terrane was developed as a result of a collisional orogenic event between mid-Permian (Guadalupian) and Late Triassic was first advanced by Mortensen (1992). Hints of a late Permian (Lopingian) metamorphic event were reported by Villeneuve et al. (2003), who dated ca. 260 Ma rims on detrital zircons in metasedimentary rocks of the western Yukon-Tanana terrane. Gordey and Ryan (2005) suggested that this Lopingian metamorphism was related to development of the penetrative S_2 transposition foliation that affects rocks of the Yukon-Tanana terrane throughout western Yukon. This interpretation was strengthened by description of the massive, post-tectonic Jim Creek pluton (ca. 252 Ma, U-Pb zircon; Figure 5c) that intruded strongly foliated, amphibolite facies carbonaceous schist of the Nasina assemblage (Figure 5a) containing ca. 260 Ma deformed sills (Beranek & Mortensen, 2011). These authors proposed that these relationships bracket the "Klondike orogeny" between ca. 260 and 252 Ma. The implication of these interpretations is that rocks deposited at surface in Guadalupian (ca. 269–260 Ma) were rapidly buried to mid-crustal levels, deformed and metamorphosed before intrusion by the Lopingian (ca. 252 Ma) Jim Creek pluton.

Berman et al. (2007) published the first quantitative thermobarometric constraints from the Yukon-Tanana terrane in western Yukon and linked these results to in situ secondary ion mass spectrometry (SIMS) U-Pb monazite dates using chemical and textural relationships. They reported monazite dates ranging from 239 to 107 Ma and moderate to high pressure and temperature (P = 0.5–1.0 GPa; T = 500–600°C) from four samples (Table 1). Samples recording Cretaceous metamorphism are restricted to a lower structural level exhumed in the Cretaceous (Staples et al., 2013) and are not further discussed here. Early Jurassic monazite (ca. 195–187 Ma) from two samples is interpreted to date metamorphism with P = 0.54–0.78 GPa and T = ~600°C (Table 1). Garnet in one of these samples contained two monazite inclusions that yielded Middle Triassic dates (ca. 239 Ma, Figure 2b); the monazite was inferred to date an earlier high pressure metamorphic event (~0.9 Gbar) that likely initiated at low pressure (Berman et al., 2007, p. 819). The sample with Triassic monazite inclusions and Early Jurassic amphibolite facies overprint is closest to the Jim Creek pluton (Figure 2b). Further east, Staples (2014) reported monazite dates from one sample (Figure 2b; Table 1). Yttrium-rich domains in monazite yielded Permian dates (ca. 264–255 Ma) while Y-poor domains are dated as Early Jurassic (ca. 197 Ma). No thermobarometric constraints were obtained from this sample.

Gaidies et al. (2021) studied three samples from the Snowcap assemblage in the Dawson Range and provided garnet Lu-Hf and Sm-Nd dates along with thermobarometric constraints (Figure 2b; Table 1). The dating of garnet, an integral phase in determination of P-T conditions, provides a direct constraint on timing of metamorphism. Two of these samples constrained the regional metamorphism and dominant foliation in this region as Early Jurassic (Lu-Hf garnet dates of ca. 192 and 188 Ma) and developed at P = 0.56–0.65 GPa and T = 560–575°C. The third sample yielded an older Middle Triassic Lu-Hf garnet date of ca. 245 Ma and an assemblage more characteristic of low P (~0.25 GPa) and high T (~710°C) conditions, typical of contact metamorphism (Table 1).

Clark (2017) provided peak metamorphic conditions of P ~7 kbar and T ~650°C for rocks assigned to the Yukon-Tanana terrane in the Aishihik region of southwestern Yukon (Figure 2b). Monazite from 7 samples in the region were analyzed by SIMS and revealed two distinct populations: (a) an older population of low-Y monazite dated ca. 194 Ma in one sample; and (b) a younger, ca. 182 Ma high-Y monazite population inferred to have grown on the retrograde path during decompression and garnet breakdown (Table 1). Although Clark (2017) describes Permian intrusions (ca. 258 Ma) that appear to crosscut a more penetrative foliation in surrounding schist, a Permian metamorphic event is not apparent in the samples analyzed in his study.

The only other recent studies of regional metamorphism in rocks assigned to the Yukon-Tanana terrane were conducted in northwestern British Columbia, >550 km south of the Klondike region (Figure 2b). Although the terrane assignment of this region is a matter of debate (e.g., Brew et al., 1994; Currie & Parrish, 1993, 1994; Mihalynuk et al., 1999), the rocks experienced a similar metamorphic evolution as the Yukon-Tanana terrane in western Yukon. Dyer (2020) reported Lu-Hf garnet dates ranging 202–185 Ma, P = 4.1–8.3 kbar and T = 500–690°C for regional metamorphic assemblages (n = 4; Table 1). Soucy La Roche et al. (2022) provided monazite and xenotime LA-ICPMS U-Pb dates for 8 samples from the same region of northwestern British Columbia. We only consider here the monazite dates for comparison with other samples summarized above. Their results are dominated by Jurassic dates (185–175 Ma) but also include monazite inclusions in garnet from two samples with

Tectonics

10.1029/2024TC008748

Table 1
Summary of Thermobarometric and Timing Constraints on Jurassic and Older Regional Metamorphism in the Western Yukon-Tanana Terrane

Sample #	Latitude	Longitude	Metamorphic assemblage[a]	*P* (GPa)	*T* (°C)	Dating method	Mineral	Age[b] (Ma)	Error (±Ma)	Comments	Source
01-VN-01	63.21589	−138.83295	Hbl-Pl-Cc-Ttn	–	–	U-Pb	Titanite	365–350	–	D1?, initial growth of titanite	Berman et al. (2007)
				–	–	U-Pb	Titanite	***~265***	–	D2?, lower intercept of discordant array	
03-RAYR-036A1	63.48293	−138.53574	Grt-Hbl-Bt-Pl-Qtz	0.98	615	–	–	–	–	D2 (?), regional metamorphism	Berman et al. (2007)
03-GGAR-175A1	63.26048	−139.84024	Grt-Hbl-Ep-Pl-Qtz	0.95	665	–	–	–	–	D2 (?), regional metamorphism	Berman et al. (2007)
03-RAY-028A1	63.70634	−139.57079	Grt-Ms-Bt-Pl-Qtz	0.9	~600	U-Pb	Monazite	***239***	***7***	D2(?), Mnz inclusion in Grt rims (n = 2); P-T estimate inferred from phase diagram	Berman et al. (2007)
				0.78	595	U-Pb	Monazite	187	5	D3, Mnz in matrix (n = 2)	
01-RAY-GR-1	63.02621	−138.58984	Grt-Ky-St-Pl-Qtz	0.54	600	U-Pb	Monazite	195	2	D3, Mnz inclusions in Grt, Ky, St (n = 7; prograde)	Berman et al. (2007)
			Grt-Ky-St-Pl-Qtz	0.76	600	–	–	–	–	D3, high-P contact metamorphism (near-peak T), Walhalla pluton (ca. 198 Ma)	
RS-09-003A	63.21655	−137.23476	Grt-Ms-Bt-Pl-Qtz	–	–	U-Pb	Monazite	***263.6***	***3.4***	Y-rich Mnz inclusion in Grt (n = 1)	Staples (2014)
				–	–	U-Pb	Monazite	***254.7***–196.8		Matrix Mnz (n = 1) with older Y-rich zone and younger Y-poor sector (range for 3 spots)	

Tectonics
10.1029/2024TC008748

Table 1
Continued

Sample #	Latitude	Longitude	Metamorphic assemblage[a]	*P* (GPa)	*T* (°C)	Dating method	Mineral	Age[b] (Ma)	Error (±Ma)	Comments	Source
15RAYJR-246A	63.32700	−140.13290	Qtz-Wm-Bt-Pl-Grt-Rt-Chl	0.56	560	Lu-Hf	Garnet	192.21	4.69	Grt—whole rock isochrons; regional metamorphism	Gaidies et al. (2021)
						Sm-Nd	Garnet	196.7	11.3		
00RAY231A	62.92010	−139.13960	Qtz-Wm-Bt-Pl-Grt-Ilm-Zrn-Gr-Chl	0.25	710	Lu-Hf	Garnet	***245.34***	***0.81***	Grt—whole rock isochrons; low-P, high-T contact metamorphism	Gaidies et al. (2021)
						Sm-Nd	Garnet	***241***	***85***		
00RAY098A	63.02480	−139.22900	Qtz-Wm-Bt-Pl-Grt-Rt-Ilm-Ap-Chl	0.65	575	Lu-Hf	Garnet	188.42	14.69	Grt—whole rock isochrons; regional metamorphism	Gaidies et al. (2021)
						Sm-Nd	Garnet	172.9	2.38		
31–07	61.03904	−137.03904	Qtz-Ky-St-Grt-Pl-Bt-Ms-Ilm-Sil	~0.7	650	U-Pb	Monazite	194.4	2.4	Matrix Mnz, rare inclusions in Grt, Ky, St; low-Y (<4,000 ppm); weighted average for 12 spots from 1 sample	Clark (2017)
20–09	61.48754	−137.44906	n/d	–	–	U-Pb	Monazite	182.2	1.2	Matrix Mnz, high-Y (>8,000 ppm) interpreted as Grt breakdown; weighted average for 29 spots from 7 samples	
77A	59.10725	−134.13938	Grt-Bt-Qtz-Wm-Pl-Rt-Py-Ccp-Ilm	0.54–0.59	510	Lu-Hf	Garnet	190.9	3.3	Grt—whole rock isochron	Dyer (2020)
			Grt	–	–	U-Pb	Monazite	185	1	Matrix Mnz (n = 66)	Soucy La Roche et al. (2022)
71	59.21777	−134.27386	Qtz-Bt-Pl-Grt-Gr-Chl	0.42–0.70	610–690	Lu-Hf	Garnet	185.4	1.1	Grt—whole rock isochron	Dyer (2020)

Tectonics
10.1029/2024TC008748

Table 1
Continued

Sample #	Latitude	Longitude	Metamorphic assemblage[a]	*P* (GPa)	*T* (°C)	Dating method	Mineral	Age[b] (Ma)	Error (±Ma)	Comments	Source
14B	59.06715	−134.02681	Qtz-Pl-Chl-Grt-Wm-Rt-Ilm	0.55	~490	Lu-Hf	Garnet	192.4	0.4	Grt—whole rock isochron	
73C	59.10599	−134.11564	Pl-Bt-Qtz-Grt-Chl-Ilm-Py-Rt-Ccp	0.41–0.83	520–555	Lu-Hf	Garnet	201.7	2.8	Grt—whole rock isochron	
25B	59.21240	−134.30307	Grt-Sil-And-Crd	–	–	U-Pb	Monazite	178	1	Matrix Mnz (n = 26), inclusions in Crd (n = 21), And (n = 11)	Soucy La Roche et al. (2022)
31	59.21889	−134.30972	(Grt)-Ky-Sil-And	–	–	U-Pb	Monazite	175	2	Matrix Mnz (n = 26), inclusions in Ky (n = 7), And (n = 15)	
67	59.26344	−134.30647	Grt	–	–	U-Pb	Monazite	176	2	Matrix Mnz (=11)	Soucy La Roche et al. (2022)
42	59.47196	−134.34311	Grt-Ky	–	–	U-Pb	Monazite	182	1	Matrix (n = 39), inclusions in Ky (n = 24), Grt (n = 2)	
46B	59.14156	−134.19394	Grt-Ky-Sil-Kfs	–	–	U-Pb	Monazite	181	1	Matrix Mnz (n = 48), inclusions in Grt (n = 14)	
83	59.10912	−134.17127	Grt-Sil-Kfs	–	–	U-Pb	Monazite	177	1	Matrix Mnz (n = 48), inclusions in Grt (n = 2)	Soucy La Roche et al. (2022)
				–	–	U-Pb	Monazite	***259***	***16***	Inclusion in Grt (n = 1)	
49B	59.14009	−134.18036	Grt-St-Ky-Sil-Crd	–	–	U-Pb	Monazite	182	1	Matrix Mnz (n = 60)	Soucy La Roche et al. (2022)
				–	–	U-Pb	Monazite	***250***	***5***	Inclusions in Grt (n = 18), low-Y	

[a]Mineral abbreviations after Kretz (1983). [b]Permian-Triassic ages inferred to relate to the "Klondike orogeny" are highlighted in bold-italics.

Permian–Triassic dates (260–250 Ma; Table 1). None of these monazite dates are, however, directly tied to thermobarometric constraints. Soucy-La Roche et al. (2022) inferred that ca. 250 Ma monazite inclusions in garnet in one sample was related to kyanite in the matrix, but matrix monazite in that and other nearby samples consistently yielded Jurassic ages consistent with PTt conditions documented by Dyer (2020) in the same region. The samples with Permian–Triassic monazite dates reported in Soucy-La Roche et al. (2022) were collected near the margin of the Wann River gneiss, a metaigneous body dated 270 ± 5 Ma (U-Pb zircon; Currie, 1992).

Early Jurassic deformation and metamorphism has also been documented in the Yukon-Tanana terrane east of the Teslin fault and in east-central Alaska (e.g., Hansen, 1992; Hansen & Dusel-Bacon, 1998; Hansen et al., 1991; Moynihan & Crowley, 2022). Mica cooling ages show that much of the Yukon-Tanana terrane was exhumed to upper crustal levels in Early to Middle Jurassic (Figure 2b; Colpron et al., 2015, 2022).

A narrow belt of Permian eclogite and blueschist marks the eastern edge of the Yukon-Tanana terrane (Figure 2) and recorded peak pressures in the range 1.5–2.3 GPa and temperatures of 500–700°C (Erdmer et al., 1998; Ghent & Erdmer, 2011; Perchuk & Philippot, 2000; Petrie et al., 2016). The timing of eclogite facies metamorphism is constrained by U-Pb zircon dates of 271–265 Ma (Creaser et al., 1997; Petrie et al., 2015, 2016) and Lu-Hf isochron ages of 264–252 Ma from a single garnet aliquot (Philippot et al., 2001). The quartzo-felspathic host rocks contain phengite that indicate they experienced similar high pressures as the eclogite (Ghent & Erdmer, 2011; Gilotti et al., 2017; Hansen, 1992; Petrie et al., 2015, 2016). Metamorphic rims on detrital zircon in the metasedimentary host rocks have U-Pb dates ca. 275–271 Ma (Gilotti et al., 2017). White mica $^{40}Ar/^{39}Ar$ dates from Permian high-pressure rocks generally range ca. 272–252 Ma suggesting rapid exhumation after metamorphism (Erdmer et al., 1998; Fallas et al., 1998). There are no indications that the high-pressure metamorphism affected rocks of the western Yukon-Tanana terrane (Read et al., 1991).

Evidence for Paleozoic deformation have been reported from various locations in the Yukon-Tanana terrane. The Snowcap assemblage has apparently experienced an older, cryptic ductile deformation event, but timing and condition of this event are not well constrained (Colpron, Mortensen, et al., 2006). In the Sylvester allochthon, a Late Devonian pluton (ca. 362 Ma) both crosscuts and is parallel to the foliation in the host rocks, indicating that deformation in this region may be as old as Devonian (Gabrielse et al., 1993). In western Yukon, ca. 365–350 Ma U-Pb titanite dates suggest that metamorphism may be as old as Late Devonian–Early Mississippian (Table 1), but the style and conditions of this event are unconstrained (Berman et al., 2007). And northeast of the Tintina fault, Lower Mississippian strata (maximum depositional age of 357 Ma) unconformably overlie folded and foliated Upper Devonian metasedimentary and metavolcanic rocks (Manor et al., 2022; Murphy et al., 2006).

A regional Viséan unconformity marks the base of the Klinkit assemblage in central and southern Yukon (Figure 3; Colpron, Mortensen, et al., 2006; Colpron, Nelson, & Murphy, 2006; Roots et al., 2006). The Klinkit assemblage overlies older strata of the Snowcap and Finlayson assemblages, and the basal conglomerate contains rare schistose clasts (Roots et al., 2006). North of Carmacks, the ca. 340 Ma Tatlmain batholith intruded foliated Early Mississippian metatonalite (ca. 347 Ma), apparently constraining the timing of a mid-Mississippian deformation in the Yukon-Tanana terrane (Colpron, Mortensen, et al., 2006).

Northeast of the Tintina fault, synorogenic clastic rocks of the lower Cisuralian (Asselian) Money Creek formation unconformably overlie folded Mississippian and Pennsylvanian strata along the eastern edge of the Yukon-Tanana terrane (Figure 3; Murphy et al., 2006). The Money Creek formation itself is folded and imbricated with the older strata, and unconformably overlain by basalt of the Cisuralian Campbell Range formation, part of the Slide Mountain terrane. These relationships provide clear indication for local folding, thrusting and juxtaposition of the Yukon-Tanana and Slide Mountain terranes in the earliest Permian (ca. 295 Ma).

Permian intrusions along the eastern edge of the Yukon-Tanana terrane, including the Ram stock in southern Yukon (ca. 263–258 Ma; Liverton et al., 2005; Roots et al., 2006; Yukon Geological Survey, 2023; Figure 2) and plutons in the upper thrust sheet of the Sylvester allochthon in northern British Columbia (ca. 264–262 Ma; Gabrielse et al., 1993; Nelson & Friedman, 2004), cut the penetrative fabric in metasedimentary rocks of the Snowcap assemblage indicating that deformation is pre-Guadalupian.

In summary, available data show that penetrative deformation and amphibolite-facies metamorphism in much of the Yukon-Tanana terrane developed in the Early Jurassic. Evidence of Paleozoic deformation has been documented in various parts of the terrane but generally predate Guadalupian–Lopingian magmatism of the Klondike assemblage. Guadalupian–Lopingian subduction-related high-pressure metamorphism and associated

Table 2
Summary of Geochronological Results for Samples Analyzed in This Study From the Klondike Region

					LA-ICPMS					CA-TIMS		
Sample	Map unit	Lithology[a]	Latitude	Longitude	N[b]	n[c]	Hf (n)	YPP[d] (Ma)	TuffZirc[e] (Ma)	n	$^{206}Pb/^{238}U$ (Ma)	±
Permian igneous rocks												
19MC-011	PJCg	Bt Granite (Jim Creek pluton)	63.807615	−139.604731	35	—	10	260	260.83 + 1.19/−2.48	6	260.84	0.07
19MC-015	PJCg	Two-mica granite (dike)	63.825469	−139.553986	36	—	10	263	263.68 + 3.86/−3.91	6	260.91	0.07
19MC-020	PSCg	Foliated metagranite (Sulphur Creek)	63.868467	−139.498816	29	—	9	250	249.50 + 2.27/−2.48	7	260.96	0.07
Klondike Schist - detrital zircon samples												
19MC-016	Psqm	Quartzite	63.960018	−139.345309	582	475	18	273	272.62 + 0.34/−0.87	_	_	_
19MC-017	Psa	Qtz-Fp schist	63.950575	−139.336909	477	341	19	248 (264)[f]	263.69 + 0.60/−0.45	12	262.25	0.06
20MC-003	Psa	Qtz-Pl-Ms schist	63.949031	−139.339039	226	67	15	262	262.38 + 0.77/−0.86	_	_	_
19MC-018	Psa/Psqm	Ms-Qtz-Pl-Chl schist	63.895336	−139.318573	520	338	26	262 (270)[f]	270.74 + 0.33/−0.44	_	_	_
19MC-021	Psq	Qtz-Ms schist	63.916888	−139.259005	595	487	21	262	262.07 + 0.42/−0.21	3	261.51	0.11

[a]Mineral abbreviations after Kretz (1983). [b]Total number of zircon analyzed. [c]Number of "acceptable dates." [d]YPP = youngest graphical peak. [e]*TuffZirc* age calculated using Isoplot 4.15 (Ludwig, 2008; Ludwig & Mundil, 2002). [f]Age in bracket corresponds to prominent peak in that sample, Figure 6.

deformation is restricted to the eastern edge of the Yukon-Tanana terrane, a structural domain that was mostly exhumed in the Lopingian. In the western Yukon-Tanana terrane, the relationships surrounding the Jim Creek pluton remain the key constraint for a ca. 260–252 Ma "Klondike orogeny."

4. Geochronology and Lu-Hf Isotopes

Eight samples of Permian (meta)igneous and metasedimentary rocks from the Klondike region were collected for U-Pb and Lu-Hf isotope analyses (Table 2). The three samples of granitoid rocks were collected to test and refine constraints on the timing of the "Klondike orogeny." Two samples are from massive ("undeformed") two-mica granite of the Jim Creek pluton and a related dike to the east (Figure 4). The other metaigneous sample is from strongly foliated granite of the Sulphur Creek orthogneiss northeast of the Ninemile thrust. All granitoid samples were analyzed by combined laser ablation inductively coupled plasma mass spectrometry (LA-ICPMS) and chemical abrasion—thermal ionization mass spectrometry (CA-TIMS) at the Isotope Geology Laboratory of Boise State University. The five samples of metaclastic rocks were collected from various map units (Table 2) to better characterize the source of metasedimentary rocks within the Klondike Schist. These samples were analyzed by LA-ICPMS for detrital zircon U-Pb at the Arizona LaserChron Center, University of Arizona. Precise determination of maximum depositional ages (MDA) for two samples of metasedimentary rocks were obtained by CA-TIMS analyses at Boise State University. Finally, Lu-Hf isotopes were measured by LA-ICPMS at the Arizona LaserChron Center for representative detrital and igneous zircons from each sample. Detailed methods for all analyses, sample descriptions, and the complete data sets are given in Colpron et al. (2025).

The presentation of detrital zircon results is focused on "acceptable dates" determined by filtering the data to exclude: (a) analyses with >10% discordance, >5% reverse discordance based on [($^{206}Pb/^{238}U$ date/$^{206}Pb/^{207}Pb$ date)—analytical error propagated at 2σ level] following equations in Gibson et al. (2021); (b) >10% 2σ analytical uncertainty of the $^{206}Pb/^{238}U$ date; and (c) >50% uncertainty of the $^{207}Pb/^{206}Pb$ date. Laser ablation ICPMS data are presented both as probability density plots (PDP) and kernel density estimates (KDE) on Figure 6. Although several methods have been proposed for the estimation of MDA from LA-ICPMS data, we only consider here the

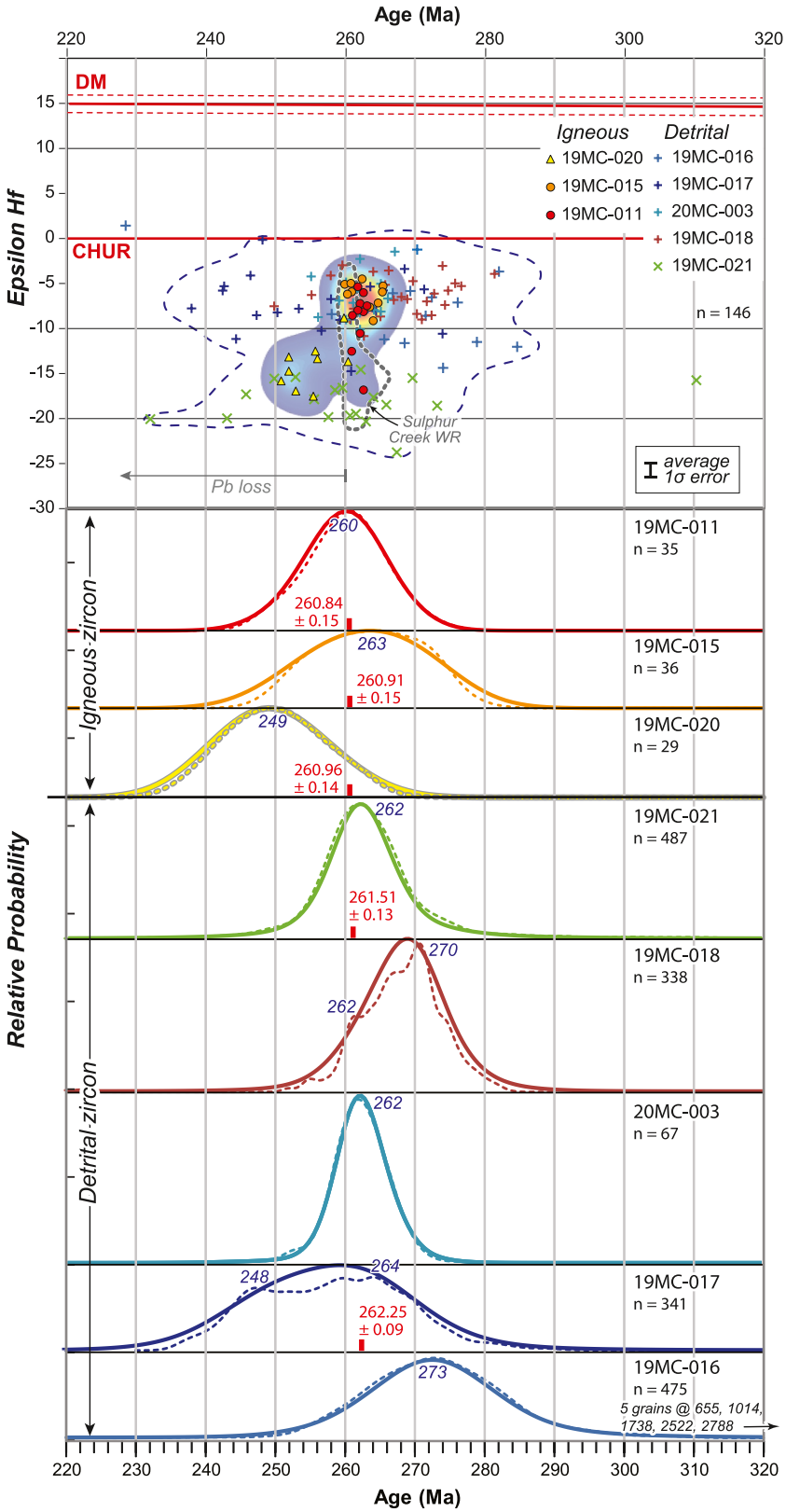
Age (Ma)
220
240
260
280
300
320
DM
CHUR
Epsilon Hf
15
10
5
0
-5
-10
-15
-20
-25
-30
Igneous
Detrital
19MC-020
19MC-015
19MC-011
19MC-016
19MC-017
20MC-003
19MC-018
19MC-021
n = 146
Sulphur Creek WR
Pb loss
average 1σ error
Relative Probability
Igneous-zircon
Detrital-zircon
260
260.84 ± 0.15
19MC-011
n = 35
263
260.91 ± 0.15
19MC-015
n = 36
249
260.96 ± 0.14
19MC-020
n = 29
262
261.51 ± 0.13
19MC-021
n = 487
270
262
19MC-018
n = 338
262
20MC-003
n = 67
248
264
262.25 ± 0.09
19MC-017
n = 341
273
19MC-016
n = 475
5 grains @ 655, 1014, 1738, 2522, 2788
220
230
240
250
260
270
280
290
300
310
320
Age (Ma)

Figure 6.

more conservative youngest graphical peak (YPP) from PDP (Figure 6) and the *TuffZirc* age calculated for this subpopulation using Isoplot 4.15 (Ludwig, 2008; Ludwig & Mundil, 2002). Our discussion of the detrital zircon results is primarily based on MDA precisely determined by CA-TIMS analysis for two samples. Those CA-TIMS MDA estimates are in good agreement with the *TuffZirc* age in these two samples, and the *TuffZirc* age is considered as MDA for the other samples (Table 2). Errors are 2σ.

4.1. Igneous Zircons

Sample 19MC-011 is a coarse-grained, unstrained biotite granite collected from the main body of the Jim Creek pluton (Figures 4 and 5c). A sample from this outcrop was previously dated at 252.4 ± 0.4 Ma by multi-grains isotope dilution—thermal ionization mass spectrometry (ID-TIMS; Beranek & Mortensen, 2011). Laser ablation ICPMS analyses on zircon from sample 19MC-011 yielded $^{206}Pb/^{238}U$ dates ranging from 269 to 249 Ma and a weighted mean of 259.6 ± 1.7 Ma for 35 analyses (Figure 6; Appendix B in Colpron et al. (2025)). Six zircons analyzed by CA-TIMS yielded $^{206}Pb/^{238}U$ dates between 260.92 ± 0.18 and 260.80 ± 0.18 Ma and a weighted mean of 260.84 ± 0.07 Ma (Figure 7; Appendix C in Colpron et al. (2025)) that is interpreted as the crystallization age of the Jim Creek pluton. Epsilon Hf_t values for zircons in sample 19MC-011 range from −5.4 to −16.8 (Figure 6; Appendix D in Colpron et al. (2025)).

Sample 19MC-015 is from a coarse-grained, two-mica, garnet-bearing granite dike east of the main body of the Jim Creek pluton. Beranek and Mortensen (2011) previously reported a $^{207}Pb/^{235}U$ monazite age of 252.5 ± 1.1 Ma from this dike. Laser ablation ICPMS analyses on zircon from sample 19MC-015 yielded $^{206}Pb/^{238}U$ dates between 275 and 251 Ma and a weighted mean of 263.1 ± 2.4 Ma ($n = 36$, Figure 6; Appendix B in Colpron et al. (2025)). Six zircons were selected for CA-TIMS and yielded $^{206}Pb/^{238}U$ dates between 261.09 ± 0.18 and 260.83 ± 0.18 Ma and a weighted mean of 260.91 ± 0.07 Ma (Figure 7; Appendix C in Colpron et al. (2025)). Epsilon Hf_t values for zircons in sample 19MC-015 range from −4.5 to −9.1 (Figure 6; Appendix D in Colpron et al. (2025)).

Sample 19MC-020 is a strongly foliated quartz-feldspar augen metagranite of the Sulphur Creek orthogneiss collected in proximity of the Ninemile thrust (Figures 4 and 5b; Table 2). Beranek and Mortensen (2011) previously reported $^{206}Pb/^{238}U$ zircon dates of 259.9 ± 0.8 Ma (ID-TIMS) and 259.0 ± 0.8 Ma (LA-ICPMS) from a sample collected at this outcrop. Laser ablation ICPMS analyses on zircon from sample 19MC-020 yielded $^{206}Pb/^{238}U$ dates ranging from 262 to 240 Ma and a weighted mean of 250.5 ± 2.3 Ma ($n = 29$, Figure 6; Appendix B in Colpron et al. (2025)). Seven zircons from this sample were analyzed by CA-TIMS and yielded $^{206}Pb/^{238}U$ dates between 261.07 ± 0.17 and 260.86 ± 0.18 Ma and a weighted mean of 260.96 ± 0.07 Ma (Figure 7; Appendix C in Colpron et al. (2025)) that is interpreted as the crystallization age of the Sulphur Creek orthogneiss. Epsilon Hf_t values for zircons in sample 19MC-020 range from −8.8 to −17.5 (Figure 6; Appendix D in Colpron et al. (2025)).

4.2. Detrital Zircons

Five samples of metaclastic rocks were collected from various map units of the Klondike Schist (Figure 4; Table 2; Mortensen, 1996). Sample 19MC-016 is a quartzite from unit Psqm of Mortensen (1996) collected along the Bonanza Creek road (Figure 4). A felsic schist from unit Psqm has an interpreted age of 263 ± 4 Ma based on discordant ID-TIMS analyses of multi-grain zircon fractions (Mortensen, 1990). Sample 19MC-016 yielded 475 acceptable dates from a total of 582 analyses with 99% of dates ranging from 367 to 237 Ma and defining a peak at 273 Ma (Figure 6; Appendix A in Colpron et al. (2025)). Five zircons yielded Precambrian ages of 2788, 2522, 1738, 1014 and 655 Ma. Epsilon Hf_t values for Paleozoic zircon in sample 19MC-016 range from −1.2 to −14.4 (Figure 6; Appendix D in Colpron et al. (2025)). Two Precambrian grains have εHf_t values of −0.5 and −2.2.

Figure 6. Kernel density estimates (KDE, solid lines), probability density plots (PDP, dotted lines) and εHf_t versus age plot (at top) for detrital and igneous zircons analyzed by LA-ICPMS in this study (Appendices A, B and D in Colpron et al. (2025)). Red bar at bottom of some KDE/PDP curves indicates CA-TIMS date from Table 2 (Appendix C in Colpron et al. (2025)). Laser ablation ICPMS dates younger than ca. 260 Ma are affected by Pb loss as discussed in the text. The field of $\varepsilon Hf_{equ.}$ calculated from whole rock Nd analyses for the Sulphur Creek suite ($n = 9$) is shown by the gray dotted line (Ruks et al., 2006; Vervoort et al., 2011). Color intensity map shows contours for εHf in igneous zircon within the 95th percentile envelope. Dashed blue line indicates the 95th percentile envelope for detrital zircon data. AgeCalcML (Sundell et al., 2021) was used to produce PDP and KDE curves. Contours of Hf data were produced with HafniumPlotter (Sundell et al., 2019). CHUR, chondrite uniform reservoir; DM, depleted mantle; WR, whole rock.

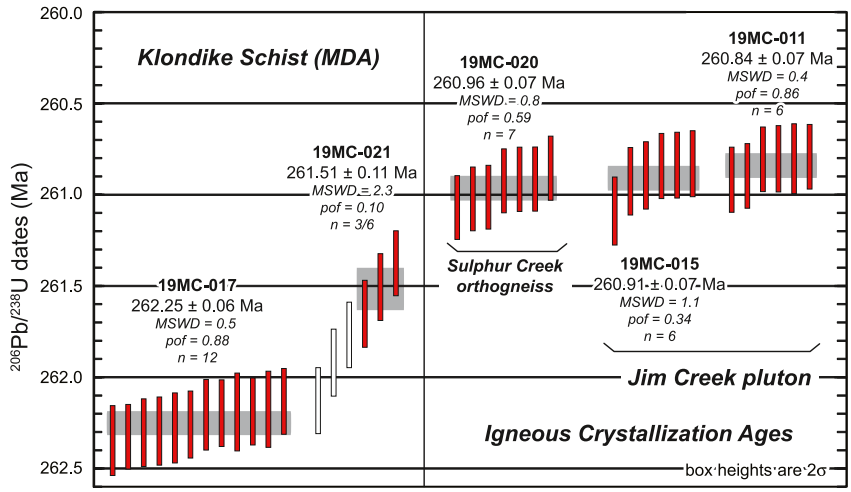

Figure 7. Ranked plots of $^{206}Pb/^{238}U$ dates for detrital and igneous zircons analyzed by CA-TIMS in this study (Table 2; Appendix C in Colpron et al. (2025)). MSWD, mean square weighted deviation; pof, probability of fit.

Sample 19MC-017 is a quartzo-feldspathic schist from unit Psa of Mortensen (1996) collected along the east side of Bonanza Creek (Figure 4; Table 2). Mortensen (1990) reported an ID-TIMS U-Pb age of 261 ± 4 Ma for multi-grain zircon fractions from a moderately foliated quartz-feldspar metaporphyry intruding unit Psa. Our sample yielded 341 acceptable analyses from a total of 477 analyses with a broad distribution of ages (ranging 367 to 236 Ma) defining two age peaks on PDP at 248 and 264 Ma (Figure 6; Appendix A in Colpron et al. (2025)). The KDE age peak for this sample is ca. 258 Ma. The youngest age peak on PDP is supported by ~27% of acceptable analyses and taken at face value would suggest an Early Triassic MDA for unit Psa of the Klondike Schist, an interpretation that is at odds with the ca. 261 Ma igneous age reported from this unit (Mortensen, 1990). To test these results, we selected 12 zircons across the range of dates obtained by LA-ICPMS and further analyzed them using the CA-TIMS method (Appendix C in Colpron et al. (2025)). All 12 grains yielded overlapping $^{206}Pb/^{238}U$ dates between 262.35 ± 0.19 and 262.14 ± 0.18 Ma and a weighted mean of 262.25 ± 0.06 Ma (Figure 7) that provides a robust MDA for unit Psa of the Klondike Schist. These results clearly show that sample 19MC-017 was subjected to significant Pb loss that was not detected by routine LA-ICPMS analyses. Epsilon Hf_t values for zircons in sample 19MC-017 range from −0.2 to −14.7 (Figure 6; Appendix D in Colpron et al. (2025)).

Another sample of metaclastic rock from unit Psa was collected on the west side of Bonanza Creek (20MC-003, Table 2), approximately 200 m southwest of locality 19MC-017 (Figure 4). Sample 20MC-003 yielded 67 acceptable dates out of 226 analyses that define a unimodal peak at 262 Ma (Figure 6; Appendix A in Colpron et al. (2025)) consistent with the MDA determined by CA-TIMS for 19MC-017. Epsilon Hf_t values for zircons in sample 20MC-003 range from −1.5 to −10.1 (Figure 6; Appendix D in Colpron et al. (2025)).

Sample 19MC-018 is a muscovite-plagioclase-quartz-garnet-chlorite schist collected at the contact between units Psa and Psqm along French Gulch (Figure 4; Table 2). It yielded 338 acceptable analyses from a total of 521 with a dominant peak at 270 Ma and lesser peak at 262 Ma(Figure 6; Appendix A in Colpron et al. (2025)). The peak in the KDE is at 268 Ma. Epsilon Hf_t values for zircons in sample 19MC-018 range from −3.0 to −10.8 (Figure 6; Appendix D in Colpron et al. (2025)).

Sample 19MC-021 is a quartz-mica schist from unit Psq, the structurally lowest unit in the Klondike Schist (Mortensen, 1996), collected along upper Bonanza Creek (Figure 4; Table 2). It yielded 487 acceptable dates from a total of 595 analyses with a unimodal peak at 262 Ma (Figure 6; Appendix A in Colpron et al. (2025)). Six zircon grains were selected for CA-TIMS analysis to precisely establish the MDA for unit Psq. They yielded $^{206}Pb/^{238}U$ dates ranging from 262.13 ± 0.18 to 261.38 ± 0.18 Ma (Appendix C in Colpron et al. (2025)). The youngest three dates have a weighted mean $^{206}Pb/^{238}U$ date of 261.51 ± 0.11 Ma and provide the MDA for this sample (Figure 7). Epsilon Hf_t values for zircons in sample 19MC-021 range from −14.6 to −23.8 (Figure 6; Appendix D in Colpron et al. (2025)).

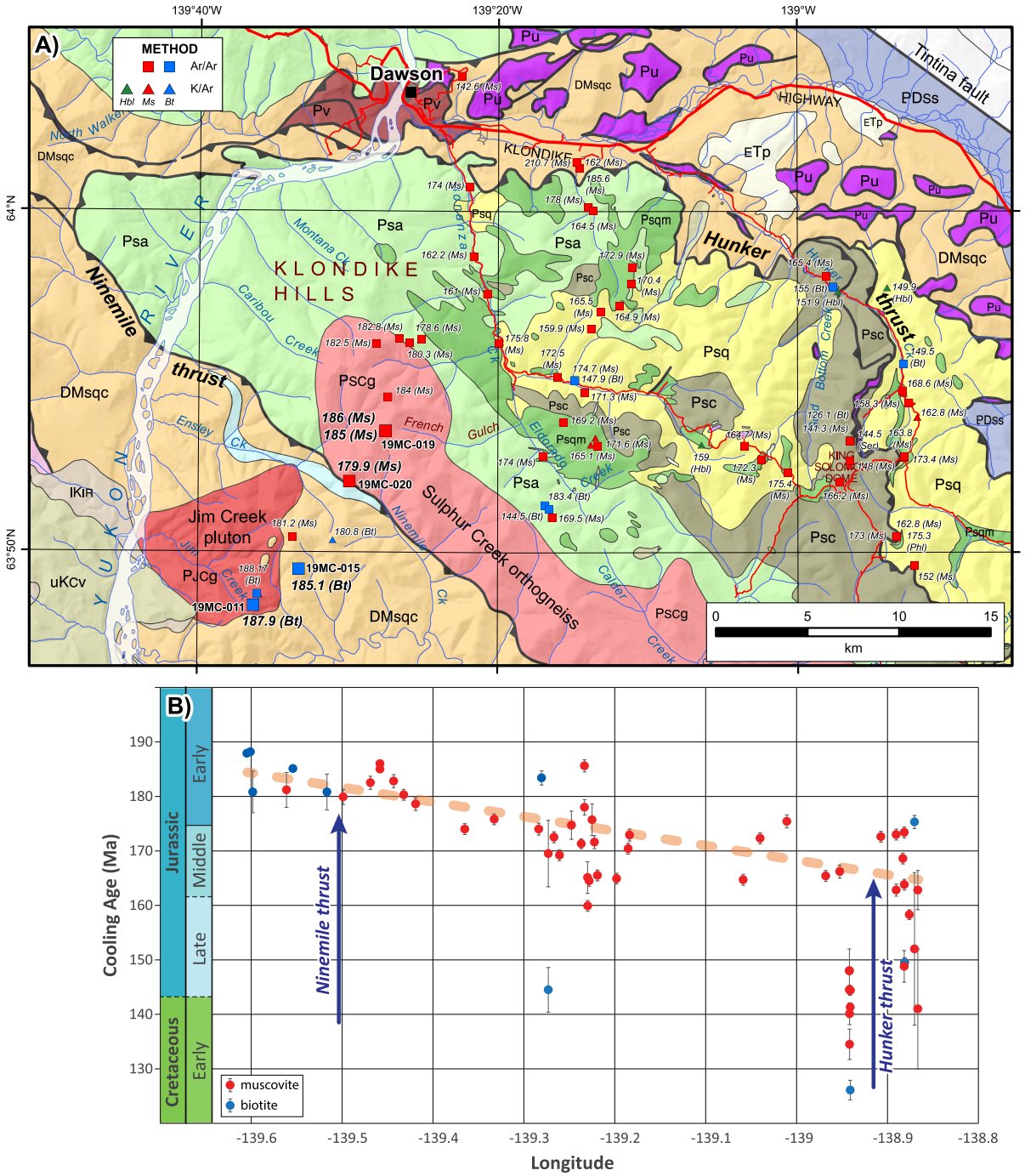

Figure 8. (a) Geological map of the Klondike region showing $^{40}Ar/^{39}Ar$ and K/Ar mica cooling ages. Larger symbols and bold types indicate samples analyzed for this study (Appendix E in Colpron et al. (2025)); all other data are from Yukon Geological Survey (2023, and sources cited therein). See Figure 4 for map legend. (b) Longitudinal transect showing younging of mica cooling ages (mostly muscovite) from west to east across the Klondike region (data from Yukon Geological Survey, 2023).

4.3. $^{40}Ar/^{39}Ar$ Thermochronology

Five aliquots of mica (2 biotite and 3 muscovite) from 4 samples of Jim Creek and Sulphur Creek plutons were analyzed using the $^{40}Ar/^{39}Ar$ step-heating method at the University of Manitoba (Appendix E in Colpron et al. (2025)) to determine the cooling ages of Permian intrusions in the region. Most samples yielded slightly disturbed age spectra with near plateau segments and integrated ages ranging ca. 190–180 Ma (see Colpron

et al., 2025). These results add to the extensive $^{40}Ar/^{39}Ar$ and K-Ar data set for the Klondike region with mica ages ranging ca. 188–140 Ma and >80% of samples yielding Jurassic cooling ages (Figure 8; Yukon Geological Survey, 2023, and sources cited therein). These results indicate that the whole Klondike region cooled below ~300–350°C in the Jurassic.

5. Whole Rock Geochemistry

Lithogeochemical data for Permian rocks of the Klondike and Dawson Range regions were compiled from various sources summarized in Colpron et al. (2025). Samples of metamorphosed Klondike Schist supracrustal rocks and Sulphur Creek plutonic rocks (including the Jim Creek pluton) were screened for alteration (see Colpron et al., 2025) and the summary of geochemical features is focused on immobile elements, including the high field strength elements (HFSE: Zr, Hf, Nb, Ta, Y, Sc), rare earth elements (REE: La-Lu), Th, V, TiO_2, and Al_2O_3. The lithogeochemistry of mafic rocks of the Dawson–Clinton Creek assemblage (van Staal et al., 2018) is also reviewed for comparison.

The Klondike Schist includes mafic, intermediate, and felsic members. The mafic rocks are subalkalic and have tholeiitic to calc-alkalic affinities (Figure 9). The tholeiitic rocks have flat trace element patterns with LREE-depletion like N-MORB (Figure 9e). The calc-alkalic suite shows a range of E-MORB to calc-alkalic trace element patterns consistent with derivation from depleted and weakly enriched mantle sources coupled with Th enrichment, typical of continental arc or continental rift settings. Intermediate and felsic rocks of the Klondike Schist have mostly calc-alkalic affinities with LREE-enriched primitive mantle normalized multi-element signatures with well-developed negative Nb and Ti anomalies and relatively flat HREE (Figure 9f). They have Nb-Y systematics consistent with I-type, volcanic arc affinities (Figure 9d).

Plutonic rocks of the Sulphur Creek suite, including the Jim Creek pluton, also comprise mafic, intermediate and felsic members. The few mafic samples are generally sub-alkalic with transitional to calc-alkalic affinities (Figure 9). Trace element patterns generally have enrichments in light rare earth elements (LREE) with negative Nb and Ti anomalies and flat to slightly depleted HREE typical of calc-alkalic rocks (Figure 9e; Pearce, 2014; Pearce & Peate, 1995). Like the calc-alkalic samples of the Klondike Schist, the Sulphur Creek mafic rocks show Th enrichment from an E-MORB parent magma common to continental arc or continental rift environments (Figure 9c). Intermediate and felsic rocks of the Sulphur Creek suite have calc-alkalic affinities with LREE-enriched primitive mantle normalized multi-element signatures, well-developed negative Nb and Ti anomalies and relatively flat HREE (Figure 9f). They have Nb-Y systematics consistent with I-type, volcanic arc affinities, like calc-alkalic samples of the Klondike Schist (Figure 9d). Plutonic rocks of the Sulphur Creek suite have evolved isotopic signatures with εNd_{260} values ranging −3 to −14 (Ruks et al., 2006).

Samples of gabbro from the Dawson–Clinton Creek assemblage were analyzed by van Staal et al. (2018). They are subalkalic with tholeiitic to calc-alkalic affinities (Figure 9). The tholeiitic suite has relatively flat trace element patterns and flat to weak negative Nb anomalies relative to Th and La, typical of N-MORB to back-arc basin basalt (BABB; e.g., Pearce & Stern, 2006). The calc-alkalic samples have LREE-enriched trace element patterns with negative Nb and Ti anomalies that are weakly developed compared to Permian mafic calc-alkalic rocks of the Klondike Schist and Sulphur Creek suite (Figure 9e). Calc-alkalic rocks of the Dawson–Clinton Creek assemblage plot along a similar trend of Th enrichment as supracrustal rocks of the Klondike Schist on the Th/Yb-Nb/Yb diagram of Pearce (2014; Figure 9c).

6. Discussion

6.1. Timing of Deposition and Magmatism in the Klondike Region

Detrital zircons from metaclastic rocks in the Klondike Schist have predominantly unimodal peaks with MDAs between 273 and 262 Ma (Figure 6; Table 2) that are consistent with local derivation from coeval volcanic and plutonic rocks (ca. 269–254 Ma; Mortensen, 1990). Precambrian zircons were recovered in only one sample suggesting minimal contributions from older components of the Yukon-Tanana terrane, or input from cratonic sources. The dominance of syn-depositional zircons in metaclastic rocks of the Klondike Schist is characteristic of deposition in a convergent margin setting (e.g., Cawood et al., 2012). Some of our detrital zircon samples yielded relatively low numbers of "acceptable" LA-ICPMS dates (30%–82% of analyzed grains; Table 2) that may reflect disturbance of the U-Pb system during deformation and metamorphism (e.g., McClelland et al., 2016). The effects

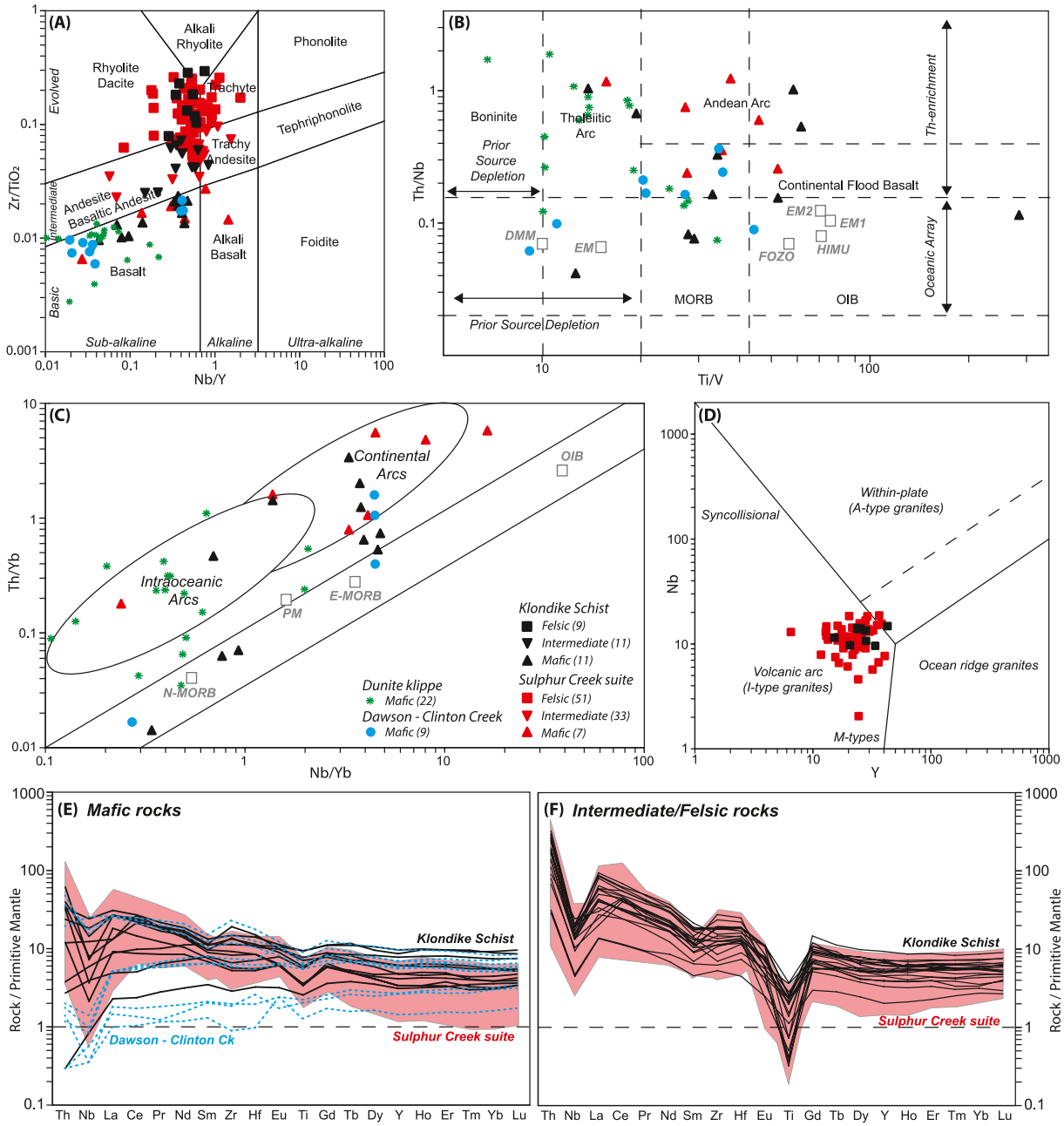

Figure 9. Trace element geochemistry of Permian rocks in the Klondike and Dawson Range regions of western Yukon (data compiled in Appendix F of Colpron et al. (2025)). (a) Zr/TiO_2-Nb/Y diagram of Pearce (1996; modified from Winchester and Floyd (1977)). (b) Th/Nb-Ti/V diagram of Shervais (2022). (c) Th/Yb-Nb/Yb diagram of Pearce (2014); updated from Pearce and Peate (1995). E-MORB, enriched mid-ocean ridge basalt; N-MORB, normal MORB; OIB, ocean island basalt. (d) Nb-Y diagram of Pearce et al. (1984). (e) Primitive mantle normalized multi-element plots for mafic rocks of the Klondike Schist and Sulphur Creek suite. (f) Primitive mantle normalized multi-element plots for intermediate and felsic rocks of the Klondike Schist and Sulphur Creek suite. Primitive mantle values from Sun and McDonough (1989). Data for the Klondike Schist, Sulphur Creek suite and Dawson–Clinton Creek assemblage are compiled in Appendix F of Colpron et al. (2025). Data for the Dunite klippe are from Parsons et al. (2019).

of Pb loss are particularly notable in sample 19MC-017 from unit Psa, which shows a broad distribution of acceptable LA-ICPMS dates between 367 ± 8 and 236 ± 2 Ma (Appendix A in Colpron et al. (2025)) with a main peak at ca. 264 Ma and a secondary peak at ca. 248 Ma (Figure 6). In this sample 71% of analyses passed the concordance filter (341 of 477 analyses; Table 2). Based on these results, the youngest peak at ca. 248 Ma could be taken as the MDA for this sample. However, a cross-cutting intrusion dated 261 ± 4 Ma constrains the minimum age of unit Psa (Mortensen, 1990). Dating of 12 zircon grains across the range of LA-ICPMS dates by

CA-TIMS yielded similar $^{206}Pb/^{238}U$ dates for all zircons and a weighted mean of 262.25 ± 0.06 Ma (Figure 7; Appendix C in Colpron et al. (2025)). This precise MDA is more consistent with the geological relationships and raises caution about interpreting MDA from LA-ICPMS analyses alone in metamorphosed sedimentary sequences. A replicate sample from unit Psa (20MC-003) yielded only 30% of acceptable analyses and a simpler age distribution with a LA-ICPMS MDA of ca. 262 Ma that is consistent with the CA-TIMS results for this unit. A precise CA-TIMS MDA was also determined for sample 19MC-021 in unit Psq. In this sample, 82% of LA-ICPMS analyses were acceptable and yielded a unimodal peak at ca. 262 Ma (Figure 6) and an equivalent CA-TIMS age of 261.51 ± 0.11 Ma (Figure 7; Appendix C in Colpron et al. (2025)). The MDA for unit Psq is younger than that of unit Psa at a higher structural level, and this may suggest that the Klondike Schist stratigraphy is overturned within the Hunker thrust sheet (Figure 4).

Precise CA-TIMS dating of the Sulphur Creek orthogneiss, which intrudes the Klondike Schist (Figure 4), and the Jim Creek pluton that intrudes Nasina assemblage to the south yielded overlapping ages of 260.96 ± 0.07 to 260.84 ± 0.07 Ma, respectively (Figure 7; Appendix C in Colpron et al. (2025)). The CA-TIMS results from the Sulphur Creek orthogneiss are comparable to previous results (multi-grain ID-TIMS and spot LA-ICPMS) of ca. 260 Ma reported by Beranek and Mortensen (2011). Interestingly, our results of LA-ICPMS analyses on sample 19MC-020 suggest a younger age of ca. 250 Ma (Figure 6) and provide evidence of Pb loss in zircons from the Sulphur Creek orthogneiss that was not previously detected.

Our results from the Jim Creek pluton present the opposite situation where previous dates of ca. 252 Ma (multi-grains ID-TIMS; Beranek & Mortensen, 2011) are younger than our more precise, single-grain CA-TIMS dates of ca. 260.9 Ma that are consistent with LA-ICPMS dates of 263–261 Ma (Figures 6 and 7). In this case, the CA-TIMS results suggests that previous dating by Beranek and Mortensen (2011) were skewed by Pb loss and provided ages that are too young.

6.2. Significance of Permian Magmatism

The geochemical character of metavolcanic rocks of the Klondike Schist indicates depleted to weakly enriched mantle sources and Th enrichment typical of continental arc or continental rift settings (Figure 9). Coeval intrusions of the Sulphur Creek suite are dominated by intermediate to felsic calc-alkalic compositions and evolved isotopic signatures (whole rock εNd_{260} −3 to −14, Ruks et al., 2006; $\varepsilon Hf_{equ.}$ −3 to −20, using the equation of Vervoort et al. (2011)) indicating melting of evolved mafic arc crust and/or contamination by sialic crust. Hafnium isotopes from igneous zircon in plutons of the Sulphur Creek suite define two distinct clusters with εHf_{260} values ranging −5 to −12 for the Jim Creek pluton and −12 to −17 for the Sulphur Creek orthogneiss that overlap whole rock values (Figure 6). The range of εHf_{260} values in magmatic rocks of the Sulphur Creek suite suggests mixing of older, evolved mafic crust with more juvenile arc crust, or underplated basalt mixed with evolved crust. It is notable that the range of εHf_{260} values in Permian magmatic rocks is comparable to Late Devonian–Early Mississippian rocks of the Finlayson assemblage (ca. 360–350 Ma; Manor et al., 2022) suggesting remelting of similar lithospheric mantle sources approximately 100 m.y. later. Similar εHf_{260} values and U-Pb ages in detrital zircons from the Klondike Schist are consistent with sources in magmatic rocks of the Sulphur Creek suite. These data are consistent with development of a magmatic arc built on, and/or rifting of, older evolved arc crust.

An alternative interpretation advanced by Parsons et al. (2019; see their figure 9) is that the Klondike magmatism resulted from orogenic collapse of an overthickened orogen in Guadalupian–Lopingian. In their model, a thick orogen developed within the Yukon-Tanana terrane in the lower plate of an east-dipping subduction zone and crustal melting occurred during extension in response to slab break-off. Our review of structural and metamorphic data and our new, precise U-Pb dating of Sulphur Creek intrusions do not support development of a metamorphic welt during a Lopingian "Klondike orogeny" (Table 1; Figure 7). Furthermore, the paucity of older age components in igneous and detrital zircons dated for this study argues against melt generation in older, sialic crust and is more consistent with a convergent margin setting. Thus, decompression melting of an overthickened orogen is not a likely mechanism for Klondike magmatism.

Slab breakoff was also proposed as a mechanism for melt generation in the Permian Klondike assemblage (Parsons et al., 2019; van Staal et al., 2018). This model would be more consistent with an upper plate position for the Yukon-Tanana terrane. Although this may explain occurrence of more primitive mafic endmembers in the Klondike Schist and the Permian exhumation of high-pressure metamorphic rocks, other geological evidence in

support of slab breakoff (such as surface uplift and sedimentation, or A-type felsic magmatism) are not evident in the Yukon-Tanana terrane (e.g., Davies & von Blanckenburg, 1995; von Blanckenburg & Davies, 1995). Change in subduction polarity is a prediction of all proposed models for evolution of the Yukon-Tanana terrane (Mortensen, 1992; Nelson et al., 2006; Parsons et al., 2019; van Staal et al., 2018); thus, slab breakoff remains a possible mechanism for triggering the Klondike magmatism in the Guadalupian–Lopingian.

Permian magmatism in the Dawson–Clinton Creek assemblage is associated with exhumation of mantle rocks in a supra-subduction zone setting, possibly as result of extension in an oceanic core complex (van Staal et al., 2018). Previous correlation of the Dawson–Clinton Creek ophiolitic rocks with those of the Slide Mountain terrane is a factor that has influenced tectonic interpretations (Colpron et al., 2016; van Staal et al., 2018; Zagorevski et al., 2021). The Slide Mountain terrane is the easternmost of the accreted terranes in the northern Cordillera (Figure 1; Monger et al., 1991). It occurs between accreted Paleozoic arc terranes (Yukon-Tanana, Quesnellia) and continental margin strata of western Laurentia, and comprises mainly supracrustal, uppermost Devonian to Cisuralian pelagic sedimentary (chert, mudstone) and mafic volcanic assemblages (e.g., Ferri, 1997; Lapierre et al., 2003; Murphy et al., 2006; Nelson, 1993; Piercey et al., 2012; Struik & Orchard, 1985). Mafic to ultramafic intrusions are comagmatic with upper Paleozoic basalt and are as young as ca. 274 Ma (Murphy et al., 2006). Ultramafic complexes (serpentinized harzburgite and peridotite) occur as distinct thrust imbricates in parts of the Slide Mountain terrane. Mafic magmatism is characterized mainly by MORB, BABB and OIB compositions (Lapierre et al., 2003; Nelson, 1993; Piercey et al., 2006, 2012).

By contrast, the Dawson–Clinton Creek assemblage occurs as thrust imbrication within the Yukon-Tanana terrane, inboard from the Slide Mountain terrane after restoration of the Tintina fault (Figure 2b). The Dawson–Clinton Creek assemblage is composed mainly of ultramafic-mafic complexes (serpentinized harzburgite-peridotite, gabbro) of exhumed mantle and only subordinate volcanic and minor sedimentary supracrustal sequences (van Staal et al., 2018). Mafic magmatism is dated ca. 265–264 Ma and mafic rocks have tholeiitic and calc-alkalic endmembers like those of the Klondike Schist. Calc-alkalic mafic rocks show similar enrichment trends as the Klondike Schist (Figure 9). Both the Klondike and Dawson–Clinton Creek assemblages are consistent with subduction zone influenced magmatism. Thus, the Dawson–Clinton Creek assemblage represents a younger (Guadalupian) ophiolitic mantle sequence that formed in a supra-subduction setting that is distinct from older (Mississippian to Cisuralian), supracrustal-dominated back-arc sequences of the Slide Mountain terrane.

Greenstone and ultramafic rocks of the ca. 268–264 Ma Dunite klippe to the south may represent yet another ophiolitic assemblage that is coeval but distinct from the Dawson–Clinton Creek assemblage. Geochemical analyses of mafic rocks from the Dunite klippe (Parsons et al., 2019) show that they are predominantly of island arc tholeiite affinity, derived from a depleted (N-MORB) mantle source, and plotting along a distinct Th enrichment trend compared to most rocks from the Dawson–Clinton Creek and Klondike assemblages (Figures 9a–9c).

6.3. Timing of Deformation and Metamorphism in the Klondike Region

The CA-TIMS results from the Jim Creek and Sulphur Creek plutons show that they are essentially the same age (Figure 7) and therefore do not bracket the timing of the "Klondike orogeny." Beranek and Mortensen (2011) suggested that the massive ca. 252 Ma Jim Creek pluton cut the penetrative foliation in the host rocks. This foliation was inferred to be part of the same deformation event that also affected ca. 260 Ma intrusions in the area, including the Sulphur Creek orthogneiss, and supracrustal rocks of the ca. 263–253 Ma Klondike Schist northeast of the Ninemile thrust (Figure 4). Gordey and Ryan (2005) and Berman et al. (2007) suggested that the dominant transposition foliation in the region developed in the Lopingian at pressures >0.8 GPa (Table 1). This would imply tectonic burial of supracrustal rocks of the Klondike assemblage to mid-crustal levels (20–25 km) within ~8 m.y. of deposition. The new CA-TIMS dates for the Jim Creek and Sulphur Creek plutons indicate (at most) a difference of 260,000 years between emplacement of these plutons, making it improbable that supracrustal rocks of the Klondike assemblage were buried to mid-crustal levels before intrusion of the Jim Creek pluton.

The Jim Creek pluton was described as massive and undeformed (Beranek & Mortensen, 2011), but we observed that the pluton experienced deformation along with the host rocks at its margins (Figure 5d). This suggests that at least part of the regional deformation in the Ninemile thrust sheet postdates emplacement of the Jim Creek pluton. The difference in fabric development between the pluton and the host metasedimentary rocks could be due to

rheological contrast where the pluton remained competent and apparently acted as a rigid body during regional deformation. This contrasts with the penetrative deformation in the coeval Sulphur Creek orthogneiss at lower structural level in the Hunker thrust sheet to the northeast. The timing of development of the penetrative foliation in rocks of the Ninemile and Hunker thrust sheets has not been directly established but has been assumed to be similar to development of the transposition foliation elsewhere in the western Yukon-Tanana terrane (e.g., Beranek & Mortensen, 2011; Gordey & Ryan, 2005; Ryan et al., 2021; Staples et al., 2016).

The review of available metamorphic data shows clear evidence that mid-crustal deformation and metamorphism in the Yukon-Tanana terrane is an Early Jurassic event (Table 1). Although part of the deformation fabric in the Yukon-Tanana terrane may have formed in the Paleozoic, available data provide few constraints on timing and conditions of older events. For samples with good age constraints tied to pressure-temperature estimates (mostly from garnet dating; Gaidies et al., 2021; Dyer, 2020), the majority indicate peak pressure (0.5–0.7 GPa) and temperatures (500–600°C) were achieved between ca. 200 and 185 Ma. This is consistent with regional evidence of Early Jurassic crustal thickening in the northern Cordillera and the timing of penetrative fabric development in the Yukon-Tanana terrane during onset of Cordilleran orogenesis (Colpron et al., 2022; Kovacs et al., 2020).

Mica cooling ages (mostly muscovite) from the Klondike region are generally Jurassic and show a trend from older ages in the hanging wall of the Ninemile thrust (ca. 190–180 Ma), in the west, to younger ages along the Hunker thrust to the east (ca. 170–160 Ma; Figure 8). Notably, both the Jim Creek and Sulphur Creek plutons, on either side of the Ninemile thrust, cooled in the Early Jurassic. The apparent younging in mica cooling ages could reflect differential exhumation across the Klondike region. Alternatively, the younger cooling ages near the Hunker thrust could be related to a Cretaceous thermal disturbance, which may be suggested by mica dates ca. 150–125 Ma in this area (Figure 8).

The only reliable PTt estimate for older, Triassic (ca. 245 Ma) metamorphism in the western Yukon-Tanana terrane suggests low P and high *T* conditions more typical of contact metamorphism (Gaidies et al., 2021). All other older, Permian–Triassic metamorphic dates are from monazite inclusions with no direct PT constraints (Table 1) and could also relate to local contact metamorphism or inheritance of igneous monazite.

We therefore suggest that the entire western Yukon-Tanana terrane was deformed at mid-crustal levels and exhumed in the Jurassic, including the Jim Creek pluton and its host rocks at higher structural levels. It remains possible that development of the foliation in the Nasina schist of the Ninemile thrust sheet predates intrusion of the Jim Creek pluton and record a Paleozoic deformation event older than Lopingian. Fabric development in the Ninemile and Hunker thrust sheets could also have occurred at different times, but the entire region was exhumed to high crustal levels by Early Jurassic.

The documentation of Permian deformation and metamorphism in the Yukon-Tanana terrane is mainly restricted to a narrow belt preserved along the eastern edge of the terrane. Northeast of the Tintina fault, Cisuralian folding and thrusting of sub-greenschsit to lower greenschist facies Carboniferous-Permian strata of the Yukon-Tanana terrane is localized to proximity of the Vangorda-Jules Creek fault and likely relate to Permian strike-slip motion along the fault (Devine et al., 2006; Murphy et al., 2006; Piercey et al., 2012).

Permian high-pressure metamorphic rocks (eclogite and blueschist) are locally preserved along the eastern edge of the Yukon-Tanana terrane (Figure 2; e.g., Erdmer et al., 1998). They were dated ca. 271–265 Ma and consist of mafic boudins within metasedimentary rocks of the Snowcap assemblage (U-Pb zircon dates; Creaser et al., 1997; Petrie et al., 2015, 2016). They were exhumed rapidly after metamorphism in the Guadalupian–Lopingian (Erdmer et al., 1998; Fallas et al., 1998). Gilotti et al. (2017) proposed that eclogite formed in slivers of upper plate arc crust entrained in the subduction channel by subduction erosion. Alternatively, the portion of the terrane affected by high-pressure metamorphism could represent a distinct crustal block within a composite Yukon-Tanana terrane (e.g., van Staal et al., 2018). In any case, the available data do not support the concept that Permian high-pressure and/or related amphibolite facies metamorphism and deformation affected the western Yukon-Tanana terrane.

6.4. Tectonic Evolution of the Yukon-Tanana Terrane

The Yukon-Tanana terrane records onset of subduction and arc magmatism along western Laurentia in latest Devonian to Early Mississippian and subsequent development of a mature Carboniferous arc system following rifting of the Slide Mountain back-arc ocean (Figures 10a and 10b; Colpron et al., 2007; Nelson et al., 2006).

Subduction was transferred from northeastern Laurentia, across the Arctic realm into Panthalassa in the Devonian, and propagated along western Laurentia following the northward drift of the craton in Early Mississippian (Cocks & Torsvik, 2011; Colpron & Nelson, 2009; Domeier & Torsvik, 2014; McClelland et al., 2021, 2022). Devonian magmatism (ca. 400–360 Ma) in the Arctic Alaska and Tracy Arm terranes probably represent earlier stages in arc development leading to Late Devonian and younger (<365 Ma) magmatism of the Yukon-Tanana terrane (Kroeger et al., 2023; Pecha et al., 2016).

The Yukon-Tanana arc was constructed above an east-dipping subduction zone (present-day coordinates) upon a metasedimentary basement rifted off western Laurentia during opening of the Slide Mountain Ocean in latest Devonian to Early Mississippian (Colpron et al., 2007; Nelson et al., 2006). Initial magmatism in Yukon-Tanana is associated with extension and involved melting of evolved lithospheric material followed by progressively more juvenile mantle components by the Late Mississippian (Kroeger et al., 2023; Manor et al., 2022). The width of the Slide Mountain Ocean remains poorly constrained, but faunal and paleomagnetic data indicate that Yukon-Tanana, Quesnellia and parts of the Slide Mountain terranes had migrated to more southern latitudes by the Cisuralian (e.g., Belasky et al., 2002; Colpron et al., 2007; Richards et al., 1993).

There is mounting evidence that the sinistral strike-slip regime established along western Laurentia in the latest Devonian controlled development of the margin throughout the late Paleozoic (Figures 10b and 10c). Provenance and tectonic analyses suggest that segments of the continental margin, the Slide Mountain (Havallah-Schoonover basin) and Northern Sierra terranes were translated southward from (present-day) British Columbia to Nevada-California in the Carboniferous (Chen & Clemens-Knott, 2021; Linde et al., 2016; Powerman et al., 2020). A series of southward younging, transtensional and flexural sedimentary basins were developed along the western Laurentian margin from Carboniferous to Guadalupian (Beranek et al., 2016; Lawton et al., 2017). These were associated with local development of northwest-southeast contractional structures, sub-regional unconformities, and southeast-directed sediment transport in the Antler basin of Nevada (e.g., Cashman & Sturmer, 2021, 2023; Trexler Jr. et al., 2004), all consistent with development along a sinistral transpressional margin. Sinistral transpression probably facilitated the southward transport of the Tracy Arm terrane, inferred to have originally developed north of the Yukon-Tanana terrane (Figure 10b). Pecha et al. (2016) suggested that southern translation of the Tracy Arm terrane (their Yukon-Tanana south) occurred in the Late Jurassic─Early Cretaceous. The occurrence of probable Yukon-Tanana-derived detrital zircons in upper Paleozoic strata of the Tracy Arm terrane suggest however possible interaction between these terranes at earlier times (Kroeger et al., 2023). The timing of juxtaposition of the Tracy Arm and Yukon-Tanana terranes is poorly constrained. Terrane interactions could be reflected in the development of the regional Viséan unconformity in the Yukon-Tanana terrane or, alternatively, may be the trigger to flip in subduction polarity in the Guadalupian (Figure 10c).

The polarity of Guadalupian–Lopingian subduction is a key difference between tectonic models. Parsons et al. (2019) and van Staal et al. (2018) proposed that parts of the Yukon-Tanana terrane were entrained in an east-dipping subduction zone to explain occurrence of high and medium pressure metamorphic rocks within the terrane. In their models, supra-subduction zone ophiolites of the Guadalupian Dawson–Clinton Creek assemblage were developed within the Slide Mountain terrane in a back-arc setting and the belt of high-pressure rocks formed between the juvenile ophiolites and the Yukon-Tanana terrane. This model does not account for the mapped distribution of these elements with eclogite-bearing Yukon-Tanana occurring east of the Dawson–Clinton Creek ophiolites and adjacent to the Cisuralian (and older) Slide Mountain terrane (Figure 2). Van Staal et al. (2018) speculated that Mesozoic contraction and extension may have resulted in wholesale reshuffling of parts of the Slide Mountain and Yukon-Tanana terranes. Although there remains much uncertainty about the development of Mesozoic structures in Yukon, there is no evidence in support of such model. Recognized stratigraphic linkages in the Slide Mountain terrane rather support the concept that it originated in its current relative position between the Yukon-Tanana terrane and the western Laurentian continental margin (*cf.*, Colpron et al., 2007, and references therein).

We prefer to consider the Permian elements of the Yukon-Tanana and Slide Mountain terranes as they occur on a Late Cretaceous palinspastic map (Figure 2b). The distribution of the main Permian tectonic elements, prior to displacement on the Tintina fault, shows the Slide Mountain terrane to the northeast, a narrow belt of eclogite along the eastern edge of the Yukon-Tanana terrane, and a belt of Permian magmatism to the southwest (Klondike/Sulphur Creek; Figure 2b). Guadalupian–Lopingian clastic rocks of the Simpson Lake Group occurs at the boundary between the Yukon-Tanana and Slide Mountain terranes and contain clasts sourced in both terranes

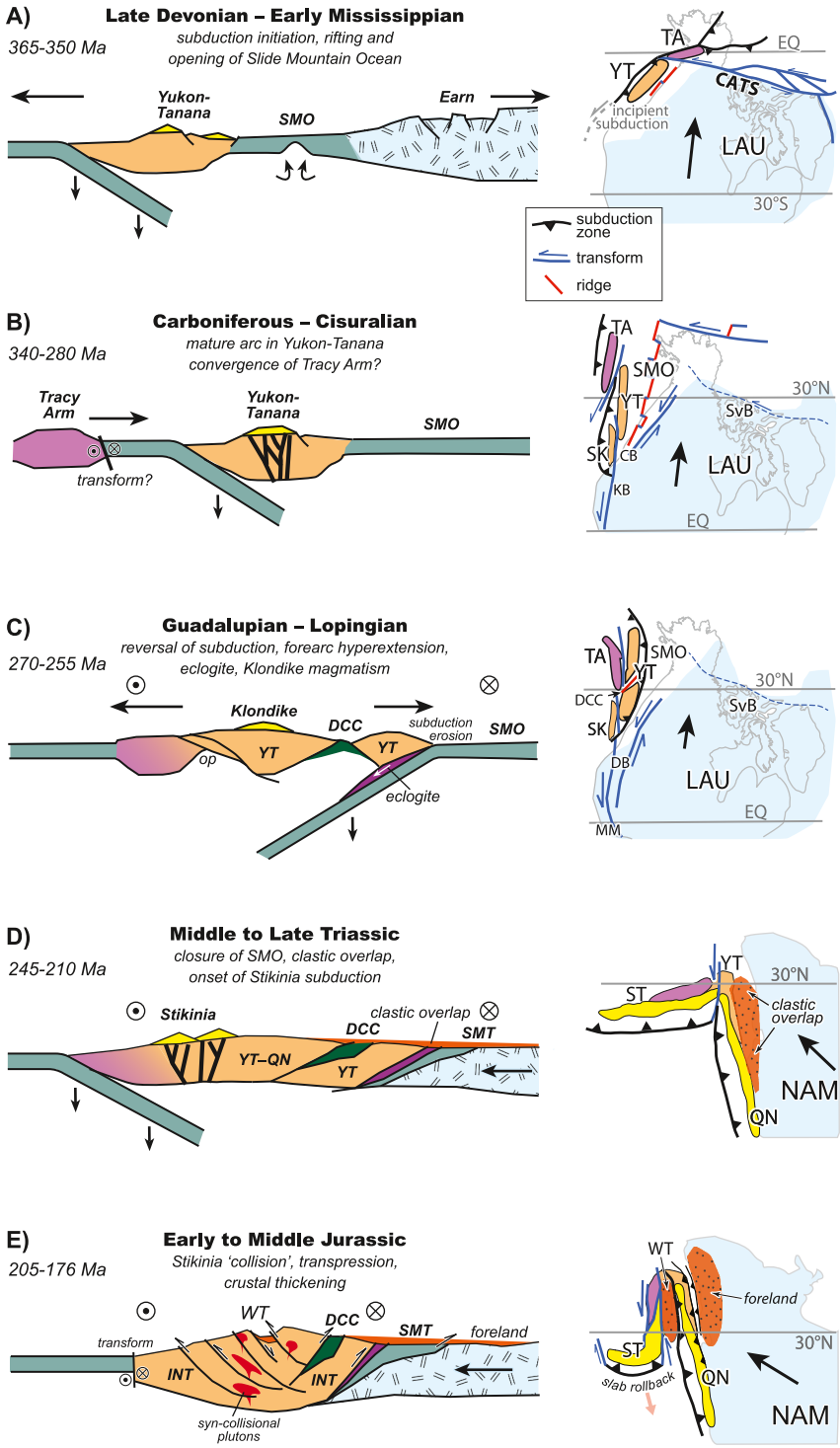
A)
Late Devonian – Early Mississippian
365-350 Ma
subduction initiation, rifting and
opening of Slide Mountain Ocean
Yukon-
Tanana
SMO
Earn
TA
EQ
YT
CATS
incipient
subduction
LAU
30°S
subduction
zone
transform
ridge
B)
Carboniferous – Cisuralian
340-280 Ma
mature arc in Yukon-Tanana
convergence of Tracy Arm?
Tracy
Arm
Yukon-
Tanana
SMO
transform?
TA
SMO
YT
30°N
SvB
SK
CB
LAU
KB
EQ
C)
Guadalupian – Lopingian
270-255 Ma
reversal of subduction, forearc hyperextension,
eclogite, Klondike magmatism
Klondike
DCC
subduction
erosion
SMO
op
YT
YT
eclogite
TA
SMO
YT
30°N
DCC
SvB
SK
DB
LAU
EQ
MM
D)
Middle to Late Triassic
245-210 Ma
closure of SMO, clastic overlap,
onset of Stikinia subduction
Stikinia
clastic overlap
DCC
SMT
YT–QN
YT
YT
30°N
ST
clastic
overlap
NAM
QN
E)
Early to Middle Jurassic
205-176 Ma
Stikinia 'collision', transpression,
crustal thickening
WT
DCC
SMT
foreland
transform
INT
INT
syn-collisional
plutons
WT
foreland
ST
30°N
slab rollback
QN
NAM

Figure 10.

(Murphy et al., 2006). Supra-subduction ophiolitic rocks of the Guadalupian Dawson–Clinton Creek assemblage occur in close association with Guadalupian–Lopingian metavolcanic and metaplutonic rocks of the Klondike assemblage, outboard of the Slide Mountain terrane (Figure 2b). This geometry forms the basis for interpreting a west-dipping Guadalupian–Lopingian subduction zone beneath the Yukon-Tanana terrane (Figure 10c; Mortensen, 1992).

The observations listed above favor an upper plate position for the Yukon-Tanana terrane in the Permian (Figure 10c). Interpretations that suggest the Yukon-Tanana terrane occupied a lower plate position are based in part on the inference that a thick orogen involving mid-crustal deformation and metamorphism was developed in the Yukon-Tanana terrane during the Lopingian "Klondike orogeny" (Parsons et al., 2019; van Staal et al., 2018). Our review of regional metamorphic data (Table 1) and new age constraints on Permian magmatism in the Klondike region (Figure 8) do not support the inference of a thick orogen in the Permian. Instead, the geological evidence is more consistent with extension of the Yukon-Tanana terrane above the subduction zone in Guadalupian to Lopingian (Figure 10c).

Subduction in the Guadalupian is indicated by formation of eclogite and blueschist ca. 271–265 Ma that were developed in slivers of Yukon-Tanana arc crust entrained by subduction erosion (Creaser et al., 1999; Gilotti et al., 2017; Petrie et al., 2015, 2016). Van Staal et al. (2018, p. 461) noted that subduction of mature oceanic crust (such as the Slide Mountain Ocean) generally results in ophiolites with little ultramafic mantle section and is commonly associated with subduction erosion. Alternatively, high-pressure metamorphic rocks formed in a distinct crustal fragment entrained in the west-dipping subduction zone, and the Yukon-Tanana terrane is a composite terrane (e.g., van Staal et al., 2018). Subduction was accompanied by hyper-extension in the upper plate and emplacement of the Dawson–Clinton Creek oceanic core complexes (ca. 265–264 Ma) and smaller orogenic peridotite massifs (ca. 267–262 Ma) within the Yukon-Tanana terrane (Figure 10c). Development of the Dawson–Clinton Creek supra-subduction ophiolite heralded magmatism of the Klondike arc (Klondike Schist and Sulphur Creek suite; ca. 265–255 Ma) as suggested by similar geochemical trends for mafic endmembers in both assemblages (Figure 9).

The Slide Mountain Ocean was closed by Middle to Late Triassic as shallow-water clastic deposits with detrital zircons sourced from the Intermontane terranes and the Laurentian craton overlap Yukon-Tanana, Slide Mountain and the continental margin (Figure 10d; Beranek & Mortensen, 2011; Beranek et al., 2010; Gabrielse, 1991; Golding et al., 2016). Closure of the Slide Mountain Ocean did not however result in a collisional orogeny as inferred in previous models (e.g., Beranek & Mortensen, 2011; Nelson et al., 2006), but rather appears to have been "soft" and was perhaps accommodated by oblique convergence along the sinistral transpressive western Laurentian margin. Sinistral transpression along the southwestern Laurentian margin appears to have resulted in intermittent deformation between the classic Late Devonian–Early Mississippian Antler and Permian–Triassic Sonoma orogenies of the western USA (Cashman & Sturmer, 2021, 2023; Lawton et al., 2017; Snyder et al., 2022; Trexler Jr. et al., 2004). Oblique closure of the Slide Mountain Ocean is consistent with these recent models of the Sonoma orogeny.

In the Middle to Late Triassic, arc magmatism of Stikinia and Quesnellia was established over a series of older Paleozoic terranes: pericratonic Yukon-Tanana in the north (Yukon and eastern Alaska; Colpron et al., 2022) and

Figure 10. Tectonic evolution of the Yukon-Tanana and related Intermontane terranes. (a) Late Devonian to Early Mississippian rifting, opening of the Slide Mountain Ocean (SMO) and onset of arc magmatism in Yukon-Tanana. (b) Late Mississippian to Cisuralian mature arc magmatism in Yukon-Tanana, continued spreading in the Slide Mountain Ocean, and convergence of the Tracy Arm terrane. (c) Guadalupian–Lopingian subduction reversal and closure of Slide Mountain Ocean. Parts of the Yukon-Tanana arc is entrained by subduction erosion, or a distinct crustal block is subducted and metamorphosed to eclogite facies (ca. 270–265 Ma). The Yukon-Tanana upper plate undergoes extension (ca. 270–265 Ma) with development of supra-subduction zone ophiolite (DCC) and emplacement of orogenic peridotite (op) in zones of hyperextension. This is followed by Klondike arc magmatism (ca. 264–258 Ma). (d) Middle to Late Triassic development of the Stikinia–Quesnellia arc system, in part on a basement of Yukon-Tanana terrane. Deposition of clastic overlap sequence on Yukon-Tanana (YT), Slide Mountain terrane (SMT) and part of the continental margin. (e) Early to Middle Jurassic onset of the Cordilleran orogeny in Yukon following collision of Stikinia and development of transpressional margin (Colpron et al., 2022). Parts of Yukon-Tanana (YT) were buried, metamorphosed and deformed at mid-crustal depths during emplacement of syn-collisional plutons in the Early Jurassic. Development of the Whitehorse trough (WT) as a strike-slip basin within the orogen was coeval with onset of foreland basin deposition to the east (Colpron et al., 2015; van Drecht et al., 2022). Abbreviations: CATS, Canadian Arctic transform system (McClelland et al., 2021); CB, Copper basin; DB, Darwin basin; DCC, Dawson–Clinton Creek assemblage; EQ, equator; INT, Intermontane terranes; KB, Keeler basin; LAU, Laurentia; MM, Mina Mexico basin; NAM, North America; QN, Quesnellia; SK, northern Sierra–eastern Klamath terrane; ST, Stikinia; SvB, Sverdrup basin; TA, Tracy Arm terrane; WT, Whitehorse trough; YT, Yukon-Tanana terrane.

distinct juvenile oceanic fragments in British Columbia (Ootes et al., 2022). The configuration of the Triassic arcs of Quesnellia and Stikinia is inferred to have been like the present-day convergence of the western Aleutian and Kamchatka subduction systems (Figure 10d; Colpron et al., 2022; George et al., 2021; Mihalynuk et al., 1994). End-on arc collision in northern Stikinia was triggered by the northwestward drift of North America during breakup of Pangea in latest Triassic (Coney, 1972; Dickinson, 2004; Monger & Gibson, 2019). This resulted in development of an orogenic welt north of the Stikine arch in Early Jurassic (Figure 1), while subduction beneath Stikinia (Hazelton arc) retreated south along a sinistral transform system (Figure 10e; Colpron et al., 2022; Nelson et al., 2022). Tectonic burial of the Yukon-Tanana terrane to mid-crustal levels occurred in the Early Jurassic and is recorded in development of the dominant tectonic fabric at pressures of 0.5–0.8 GPa and temperatures of 500–700°C (Table 1). Much of the Yukon-Tanana terrane was exhumed to upper crustal levels ($T \leq 300$°C) in the Early to Middle Jurassic (Figures 2b and 8; Colpron et al., 2022). Exhumation was associated with emplacement of syn-collisional plutons and development of the synorogenic Whitehorse trough in the northern Cordillera (Colpron et al., 2015, 2022; van Drecht et al., 2022). The Early Jurassic convergence of the Intermontane terranes with western North America is recorded in early subsidence of the Canadian foreland basin in Alberta (Colpron et al., 2015; Pană et al., 2018).

7. Conclusions

The Permian Klondike assemblage of the Yukon-Tanana terrane records magmatism emplaced in a supra-subduction setting during closure of the Slide Mountain Ocean. A review of metamorphic data from the western Yukon-Tanana terrane indicates that mid-crustal deformation and metamorphism thought to relate with the Lopingian "Klondike orogeny" is more consistent with crustal thickening associated with the Early Jurassic accretion of the Intermontane terranes in the northern Cordillera. Precise CA-TIMS dating of zircon in (meta)igneous rocks inferred to constrain the timing of the "Klondike orogeny" (ca. 260–252 Ma) shows that all plutonic bodies in the Klondike region have similar ages of ca. 260.9 Ma and that previous dating was affected by unmitigated Pb loss. Using the combination of LA-ICPMS and CA-TIMS U-Pb zircon dating methods allows identification of Pb loss in metamorphic rocks of the Klondike region and raises caution about interpretation of U-Pb zircon results in metamorphic terranes. Sinistral transpression along the western Laurentian margin facilitated development of the Yukon-Tanana terrane and subsequent orogenic activity from Paleozoic to early Mesozoic. Sinistral transpression probably linked the closure of the Slide Mountain Ocean with intermittent late Paleozoic deformation culminating in the Sonoma orogeny of the U.S. Cordillera.

Data Availability Statement

Uranium-lead geochronological data, Lu-Hf isotopic data, $^{40}Ar/^{39}Ar$ data, and a compilation of lithogeochemical data used to develop interpretations presented in this article are available for download from Colpron et al. (2025, https://data.geology.gov.yk.ca/Reference/96117).

Acknowledgments
This paper is dedicated to the memory of Ray Price (1933–2024) who first introduced MC to the conundrums of Cordilleran geology. This study was funded by the Yukon Geological Survey. Discussions with Jim Monger, Don Murphy, JoAnne Nelson and many other Cordilleran colleagues have influenced development of ideas. Matt Manor and Craig Hart participated is some of the field work for this study. JoAnne Nelson commented on an early version of the manuscript. Comments by Andy Parsons and an anonymous reviewer helped improve the paper. This is Yukon Geological Survey contribution #077.

References

Bazard, D. R., Butler, R. F., Gehrels, G. E., & Soja, C. M. (1995). Early Devonian paleomagnetic data from the Lower Devonian Karheen Formation suggest Laurentia-Baltica connection for the Alexander terrane. *Geology*, *23*(8), 707–710. https://doi.org/10.1130/0091-7613(1995)023<0707:edpdft>2.3.co;2

Belasky, P., Stevens, C. H., & Hanger, R. A. (2002). Early Permian location of western North American terranes based on brachiopod, fusulinid and coral biogeography. *Palaeogeography, Palaeoclimatology, Palaeoecology*, *179*(3–4), 245–266. https://doi.org/10.1016/s0031-0182(01)00437-0

Beranek, L. P., Link, P. K., & Fanning, C. M. (2016). Detrital zircon record of mid-Paleozoic convergent margin activity in the northern U.S. Rocky Mountains: Implications for the Antler orogeny and early evolution of the North American Cordillera. *Lithosphere*, *8*(5), 533–550. https://doi.org/10.1130/l557.1

Beranek, L. P., & Mortensen, J. K. (2011). The timing and provenance record of the Late Permian Klondike orogeny in northwestern Canada and arc-continent collision along western North America. *Tectonics*, *30*(23), TC5017. https://doi.org/10.1029/2010TC002849

Beranek, L. P., Mortensen, J. K., Orchard, M. J., & Ullrich, T. (2010). Provenance of North American Triassic strata from west-central and southeastern Yukon: Correlations with coeval strata in the Western Canada Sedimentary Basin and Canadian Arctic Islands. *Canadian Journal of Earth Sciences*, *47*(1), 53–73. https://doi.org/10.1139/e09-065

Berman, R. G., Ryan, J. J., Gordey, S. P., & Villeneuve, M. (2007). Permian to Cretaceous polymetamorphic evolution of the Stewart River region, Yukon-Tanana terrane, Yukon, Canada: P–T evolution linked with *in situ* SHRIMP monazite geochronology. *Journal of Metamorphic Geology*, *25*(7), 803–827. https://doi.org/10.1111/j.1525-1314.2007.00729.x

Brew, D. A., Ford, A. B., Himmelberg, G. R., Currie, L., & Parrish, R. R. (1994). Jurassic accretion of Nisling terrane along the western margin of Stikinia, Coast Mountains, northwestern British Columbia – Comment. *Geology*, *22*(1), 89–90. https://doi.org/10.1130/0091-7613(1994)022<0089:jaonta>2.3.co;2

Cashman, P. H., & Sturmer, D. M. (2023). The Antler orogeny reconsidered and implications for late Paleozoic tectonics of western Laurentia. *Geology*, *51*(6), 543–548. https://doi.org/10.1130/G50977.1

Cashman, P. H., & Sturmer, D. M. (2021). Paleogeographic reconstruction of Mississippian to Middle Pennsylvanian basins in Nevada, southwestern Laurentia. *Palaeogeography, Palaeoclimatology, Palaeoecology*, *584*, 110666. https://doi.org/10.1016/j.palaeo.2021.110666

Cawood, P. A., Hawkesworth, C. J., & Dhuime, B. (2012). Detrital zircon record and tectonic setting. *Geology*, *40*(10), 875–878. https://doi.org/10.1130/g32945.1

Chen, N. M., & Clemens-Knott, D. (2021). Detrital zircon uranium-lead geochronology of the Schoonover Sequence (Golconda Allochthon, Nevada): Alternative paleogeography of the Havallah-Schoonover Basin with implications for Antler-SLaB-Sonoma orogenesis. *Palaeogeography, Palaeoclimatology, Palaeoecology*, *575*, 110471. https://doi.org/10.1016/j.palaeo.2021.110471

Clark, A. D. (2017). *Tectonometamorphic history of mid-crustal rocks at Aishihik Lake, southwest Yukon* (M.Sc. thesis). Simon Fraser University.

Cobbett, R., Colpron, M., Crowley, J. L., Cordey, F., Blodgett, R. B., & Orchard, M. J. (2021). Late Devonian magmatism and clastic deposition in the upper Earn Group (central Yukon) mark the transition from passive to active margin along western Laurentia. *Canadian Journal of Earth Sciences*, *58*(5), 471–494. https://doi.org/10.1139/cjes-2020-0161

Cocks, L. R. M., & Torsvik, T. H. (2011). The Palaeozoic geography of Laurentia and western Laurussia: A stable craton with mobile margins. *Earth-Science Reviews*, *106*(1–2), 1–51. https://doi.org/10.1016/j.earscirev.2011.01.007

Colpron, M., Crowley, J. L., Gehrels, G. E., Long, D. G. F., Murphy, D. C., Beranek, L. P., & Bickerton, L. (2015). Birth of the northern Cordilleran orogen, as recorded by detrital zircons in Jurassic synorogenic strata and regional exhumation in Yukon. *Lithosphere*, *7*(5), 541–562. https://doi.org/10.1130/l451.1

Colpron, M., Gladwin, K., Johnston, S. T., Mortensen, J. K., & Gehrels, G. E. (2005). Geology and juxtaposition history of Yukon-Tanana, Slide Mountain and Cassiar terranes in the Glenlyon area of central Yukon. *Canadian Journal of Earth Sciences*, *42*(8), 1431–1448. https://doi.org/10.1139/e05-046

Colpron, M., Israel, S., Murphy, D. C., Pigage, L. C., & Moynihan, D. (2016). *Yukon Bedrock Geology Map* (Open File 2016-1). Yukon Geological Survey.

Colpron, M., McClelland, W. C., Kroeger, E. D. L., Piercey, S. J., Crowley, J. L., & Gehrels, G. E. (2025). New geochronological and geochemical data for Permian rocks of the western Yukon-Tanana terrane, Klondike district, Yukon (Open File 2025-4) [Dataset]. *Yukon Geological Survey*. https://data.geology.gov.yk.ca/Reference/96117

Colpron, M., Mortensen, J. K., Gehrels, G. E., & Villeneuve, M. E. (2006). Basement complex, Carboniferous magmatism and Paleozoic deformation in Yukon-Tanana terrane of central Yukon: Field, geochemical and geochronological constraints from Glenlyon map area. In M. Colpron & J. L. Nelson (Eds.), *Paleozoic Evolution and Metallogeny of Pericratonic Terranes at the Ancient Pacific Margin of North America, Canadian and Alaskan Cordillera*, *Special Paper* (Vol. 45, pp. 131–151). Geological Association of Canada.

Colpron, M., & Nelson, J. L. (2009). A Palaeozoic Northwest Passage: Incursion of Caledonian, Baltican and Siberian terranes into eastern Panthalassa, and the early evolution of the North American Cordillera. In P. A. Cawood & A. Kröner (Eds.), *Earth Accretionary Systems in Space and Time*, *Special Publications* (Vol. 318, pp. 273–307). Geological Society of London.

Colpron, M., & Nelson, J. L. (2011). A Palaeozoic Northwest Passage and the Timanian, Caledonian and Uralian connections of some exotic terranes in the North American Cordillera, Chapter 31. In A. M. Spencer, A. Embry, D. Gautier, A. Stoupakova, & K. Sørensen (Eds.), *Arctic Petroleum Geology. Memoirs* (Vol. 35, pp. 463–484). Geological Society of London.

Colpron, M., & Nelson, J. L. (2021). Northern Cordillera: Canada and Alaska. In S. A. Elias & D. Alderton (Eds.), *Encyclopedia of Geology*, *Reference Module in Earth Systems and Environmental Sciences* (2nd ed., pp. 93–106). Elsevier.

Colpron, M., Nelson, J. L., & Murphy, D. C. (2006). A tectonostratigraphic framework for the pericratonic terranes of the northern Cordillera. In M. Colpron & J. L. Nelson (Eds.), *Paleozoic Evolution and Metallogeny of Pericratonic Terranes at the Ancient Pacific Margin of North America, Canadian and Alaskan Cordillera*, *Special Paper* (Vol. 45, pp. 1–23). Geological Association of Canada.

Colpron, M., Nelson, J. L., & Murphy, D. C. (2007). Northern Cordilleran terranes and their interactions through time. *GSA Today*, *17*(4/5), 4–10. https://doi.org/10.1130/gsat01704-5a.1

Colpron, M., & Ryan, J. J. (2010). Bedrock geology of southwest McQuesten (NTS 115P) and part of northern Carmacks (NTS 115I) map area. In K. E. MacFarlane, L. H. Weston, & L. R. Blackburn (Eds.), *Yukon Exploration and Geology 2009* (pp. 159–184). Yukon Geological Survey.

Colpron, M., Sack, P. J., Crowley, J. L., Beranek, L. P., & Allan, M. M. (2022). Late Triassic to Jurassic magmatic and tectonic evolution of the Intermontane terranes in Yukon, northern Canadian Cordillera: Transition from arc to syn-collisional magmatism and post-collisional lithospheric delamination. *Tectonics*, *41*(2), e2021TC007060. https://doi.org/10.1029/2021TC007060

Coney, P. J. (1972). Cordilleran tectonics and North American plate motions. *American Journal of Science*, *272*(7), 603–628. https://doi.org/10.2475/ajs.272.7.603

Coney, P. J., Jones, D. L., & Monger, J. W. H. (1980). Cordilleran suspect terranes. *Nature*, *288*(5789), 329–333. https://doi.org/10.1038/288329a0

Creaser, R. A., Goodwin-Bell, J. S., & Erdmer, P. (1999). Geochemical and Nd isotopic constraints for the origin of eclogite protoliths, northern Cordillera: Implications for the Paleozoic tectonic evolution of the Yukon-Tanana terrane. *Canadian Journal of Earth Sciences*, *36*(10), 1697–1709. https://doi.org/10.1139/cjes-36-10-1697

Creaser, R. A., Heaman, L. M., & Erdmer, P. (1997). Timing of high-pressure metamorphism in the Yukon-Tanana terrane, Canadian Cordillera: Constraints from U-Pb zircon dating of eclogite from the Teslin tectonic zone. *Canadian Journal of Earth Sciences*, *34*(5), 709–715. https://doi.org/10.1139/e17-057

Cui, Y., Miller, D., Schiarizza, P., & Diakow, L. J. (2017). *British Columbia digital geology* (Open File 2017-8). British Columbia Ministry of Energy, Mines and Petroleum Resources, British Columbia Geological Survey.

Currie, L., & Parrish, R. R. (1994). Jurassic accretion of Nisling terrane along the western margin of Stikinia, Coast Mountains, northwestern British Columbia – Reply. *Geology*, *22*, 90.

Currie, L. D. (1992). Metamorphic rocks in the Tagish Lake area, northern Coast Mountains, British Columbia: A possible link between Stikinia and parts of Yukon-Tanana terrane. In *Current Research, Part A* (Paper 92-1A) (pp. 199–208). Geological Survey of Canada.

Currie, L. D., & Parrish, R. R. (1993). Jurassic accretion of Nisling terrane along the western margin of Stikinia, Coast Mountains, northwestern British Columbia. *Geology*, *21*(3), 235–238. https://doi.org/10.1130/0091-7613(1993)021<0235:jaonta>2.3.co;2

Davies, J. H., & von Blanckenburg, F. (1995). Slab breakoff: A model of lithosphere detachment and its test in the magmatism and deformation of collisional orogens. *Earth and Planetary Science Letters*, *129*(1–4), 85–102. https://doi.org/10.1016/0012-821x(94)00237-s

Devine, F., Carr, S. D., Murphy, D. C., Davis, W. J., Smith, S., & Villeneuve, M. E. (2006). Geochronological and geochemical constraints on the origin of the Klatsa metamorphic complex: Implications for Early Mississippian high-pressure metamorphism within Yukon-Tanana terrane. In M. Colpron & J. L. Nelson (Eds.), *Paleozoic Evolution and Metallogeny of Pericratonic Terranes at the Ancient Pacific Margin of North America, Canadian and Alaskan Cordillera*, *Special Paper* (Vol. 45, pp. 107–130). Geological Association of Canada.

Dickinson, W. R. (2004). Evolution of the North American Cordillera. *Annual Reviews of Earth and Planetary Science*, *32*(1), 13–45. https://doi.org/10.1146/annurev.earth.32.101802.120257

Domeier, M., & Torsvik, T. H. (2014). Plate tectonics in the late Paleozoic. *Geoscience Frontiers*, *5*(3), 303–350. https://doi.org/10.1016/j.gsf.2014.01.002

Dusel-Bacon, C., & Cooper, K. M. (1999). Trace-element geochemistry of metabasaltic rocks from the Yukon–Tanana Upland and implications for the origin of tectonic assemblages in east-central Alaska. *Canadian Journal of Earth Sciences*, *36*(10), 1671–1695. https://doi.org/10.1139/cjes-36-10-1671

Dusel-Bacon, C., Holm-Denoma, C. S., Jones, J. V., III, Aleinikoff, J. N., & Mortensen, J. K. (2017). Detrital zircon geochronology of quartzose metasedimentary rocks from parautochthonous North America, east-central Alaska. *Lithosphere*, *9*(6), 927–952. https://doi.org/10.1130/L672.1

Dusel-Bacon, C., Hopkins, M. J., Mortensen, J. K., Dashevsky, S. S., Bressler, J. R., & Day, W. C. (2006). Paleozoic tectonic and metallogenic evolution of the pericratonic rocks of east-central Alaska and adjacent Yukon. In M. Colpron & J. L. Nelson (Eds.), *Paleozoic Evolution and Metallogeny of Pericratonic Terranes at the Ancient Pacific Margin of North America, Canadian and Alaskan Cordillera*, *Special Paper* (Vol. 45, pp. 25–74). Geological Association of Canada.

Dusel-Bacon, C., Lanphere, M. A., Sharp, W. D., Layer, P. W., & Hansen, V. L. (2002). Mesozoic thermal history and timing of structural events for the Yukon-Tanana Upland, east-central Alaska: $^{40}Ar/^{39}Ar$ data from metamorphic and plutonic rocks. *Canadian Journal of Earth Sciences*, *39*(6), 1013–1051. https://doi.org/10.1139/e02-018

Dusel-Bacon, C., & Mortensen, J. K. (2023). *New U-Pb geochronology and geochemistry of Paleozoic metaigneous rocks from western Yukon and eastern Alaska* (Data release). U.S. Geological Survey. https://doi.org/10.5066/P93ZWGA1

Dusel-Bacon, C., & Mortensen, J. K. (2024). *New U-Pb geochronology and geochemistry of Paleozoic metaigneous rocks from western Yukon and eastern Alaska, cross-border synthesis, and implications for tectonic models* (Professional Paper 1888). U.S. Geological Survey. https://doi.org/10.3133/pp1888

Dyer, S. (2020). *The Early Jurassic metamorphic history of the Yukon-Tanana terrane of northwestern British Columbia: Insights from a new inverse garnet fractionation modelling technique* (M.Sc. thesis). Carleton University.

Erdmer, P., Ghent, E. D., Archibald, D. A., & Stout, M. Z. (1998). Paleozoic and Mesozoic high-pressure metamorphism at the margin of ancestral North America in central Yukon. *Geological Society of America Bulletin*, *110*(5), 615–629. https://doi.org/10.1130/0016-7606(1998)110<0615:pamhpm>2.3.co;2

Fallas, K. M., Erdmer, P., Archibald, D. A., Heaman, L., & Creaser, R. (1998). The St. Cyr klippe, south-central Yukon: An outlier of the Teslin tectonic zone? In F. Cook & P. Erdmer (Eds.), *Slave-Northern Cordillera Lithospheric Evolution (SNORCLE) Transect and Cordilleran Tectonic Workshop*, *Lithoprobe Report* (Vol. 64, pp. 131–138). Simon Fraser University. Retrieved from https://data.geology.gov.yk.ca/Reference/96085

Ferri, F. (1997). Nina Creek Group and Lay Range Assemblage, north-central British Columbia: Remnants of late Paleozoic oceanic and arc terranes. *Canadian Journal of Earth Sciences*, *34*(6), 854–874. https://doi.org/10.1139/e17-070

Gabrielse, H. (1985). Major dextral transcurrent displacements along the northern Rocky Mountain Trench and related lineaments in north-central British Columbia. *Geological Society of America Bulletin*, *96*, 1–14. https://doi.org/10.1130/0016-7606(1985)96<1:mdtdat>2.0.co;2

Gabrielse, H. (1991). Late Paleozoic and Mesozoic terrane interactions in north-central British Columbia. *Canadian Journal of Earth Sciences*, *28*(6), 947–957. https://doi.org/10.1139/e91-086

Gabrielse, H., Mortensen, J. K., Parrish, R. R., Harms, T. A., Nelson, J. L., & van der Heyden, P. (1993). Late Paleozoic plutons in the Sylvester Allochthon, northern British Columbia. Paper 93-2. In *Radiogenic Age and Isotopic Studies: Report 7* (pp. 107–118). Geological Survey of Canada.

Gabrielse, H., Murphy, D. C., & Mortensen, J. K. (2006). Cretaceous and Cenozoic dextral orogen-parallel displacements, magmatism and paleogeography, north-central Canadian Cordillera. In J. W. Haggart, J. W. H. Monger, & R. J. Enkin (Eds.), *Paleogeography of the North American Cordillera: Evidence for and against large-scale displacements*, *Special Paper* (Vol. 46, pp. 255–276). Geological Association of Canada.

Gaidies, F., Morneau, Y. E., Petts, D. C., Jackson, S. E., Zagorevski, A., & Ryan, J. J. (2021). Major and trace element mapping of garnet: Unravelling the conditions, timing and rates of metamorphism of the Snowcap assemblage, west-central Yukon. *Journal of Metamorphic Geology*, *39*(2), 133–164. https://doi.org/10.1111/jmg.12562

Gehrels, G. E., McClelland, W. C., Samson, S. D., Patchett, P. J., & Jackson, J. L. (1990). Ancient continental margin assemblage in the northern Coast Mountains, southeast Alaska and northwest Canada. *Geology*, *18*(3), 208–211. https://doi.org/10.1130/0091-7613(1990)018<0208:acmait>2.3.co;2

Gehrels, G. E., McClelland, W. C., Samson, S. D., Patchett, P. J., & Orchard, M. J. (1992). Geology of the western flank of the Coast Mountains between Cape Fanshaw and Taku Inlet, southeastern Alaska. *Tectonics*, *11*(3), 567–585. https://doi.org/10.1029/92tc00482

George, S. W. M., Nelson, J. L., Alberts, D., Greig, C. J., & Gehrels, G. E. (2021). Triassic–Jurassic accretionary history and tectonic origins of Stikinia from U-Pb geochronology and Lu-Hf isotope analysis, British Columbia. *Tectonics*, *40*(4), e2020TC006505. https://doi.org/10.1029/2020TC006505

Ghent, E., & Erdmer, P. (2011). Very high-pressure epidote eclogite from Ross River area, Yukon, Canada, records deep subduction. In L. F. Dobrzhinetskaya, S. W. Faryad, S. Wallis, & S. Cuthbert (Eds.), *Ultrahigh pressure metamorphism 25 years after the discovery of coesite and diamond* (pp. 279–290). Elsevier.

Gibson, T. M., Faehnrich, K., Busch, J. F., McClelland, W. C., Schmitz, M. D., & Strauss, J. V. (2021). A detrital zircon test of large-scale terrane displacement along the Arctic margin of North America. *Geology*, *49*(5), 545–550. https://doi.org/10.1130/G48336.1

Gilotti, J. A., McClelland, W. C., van Staal, C. R., & Petrie, M. B. (2017). Detrital zircon evidence for eclogite formation by basal subduction erosion – An example from the Yukon-Tanana composite arc, Canadian Cordillera. In G. Bianchini, J.-L. Bodinier, R. Braga, & M. Wilson (Eds.), *The Crust-Mantle and Lithosphere-Asthenosphere Boundaries: Insights from Xenoliths, Orogenic Deep Sections, and Geophysical Studies*, *Special Paper* (Vol. 526, pp. 173–189). Geological Society of America.

Golding, M. L., Mortensen, J. K., Ferri, F., Zonneveld, J.-P., & Orchard, M. J. (2016). Determining the provenance of Triassic sedimentary rocks in northeastern British Columbia and western Alberta using detrital zircon geochronology, with implications for regional tectonics. *Canadian Journal of Earth Sciences*, *53*(2), 140–155. https://doi.org/10.1139/cjes-2015-0082

Gordey, S. P. (2013). *Evolution of the Selwyn Basin region, Sheldon Lake (105J) and Tay River (105K) map areas, central Yukon Territory* (Bulletin 599). Geological Survey of Canada.

Gordey, S. P., Abbott, J. G., Tempelman-Kluit, D. J., & Gabrielse, H. (1987). "Antler" elastics in the Canadian Cordillera. *Geology*, *15*(2), 103–107. https://doi.org/10.1130/0091-7613(1987)15<103:aeitcc>2.0.co;2

Gordey, S. P., & Anderson, R. G. (1993). *Evolution of the northern Cordilleran miogeocline, Nahanni map area (105I), Yukon and Northwest Territories* (Memoir 428). Geological Survey of Canada.

Gordey, S. P., & Makepeace, A. J. (2001). *Bedrock geology, Yukon Territory* (Open File 3754). Geological Survey of Canada.

Gordey, S. P., & Ryan, J. J. (2005). *Geology, Stewart River area (115N, 115O and part of 115J), Yukon Territory* (Open File 4970). Geological Survey of Canada.

Han, T., Ootes, L., & Yun, K. (2020). *The new British Columbia Geological Survey geochronologic database: Preliminary release of ages* (GeoFile 2020-10). British Columbia Ministry of Energy, Mines and Petroleum Resources.

Hansen, V. L. (1992). *P-T* evolution of the Teslin suture zone and Cassiar tectonites, Yukon, Canada: Evidence for A- and B-type subduction. *Journal of Metamorphic Geology*, *10*(2), 239–263. https://doi.org/10.1111/j.1525-1314.1992.tb00081.x

Hansen, V. L., & Dusel-Bacon, C. (1998). Structural and kinematic evolution of the Yukon-Tanana upland tectonites, east-central Alaska: A record of late Paleozoic to Mesozoic crustal assembly. *Geological Society of America Bulletin*, *110*(2), 211–230. https://doi.org/10.1130/0016-7606(1998)110<0211:sakeot>2.3.co;2

Hansen, V. L., Heizler, M. T., & Harrison, T. M. (1991). Mesozoic thermal evolution of the Yukon-Tanana composite terrane: New evidence from $^{40}Ar/^{39}Ar$ data. *Tectonics*, *10*(1), 51–76. https://doi.org/10.1029/90tc01930

Johnston, S. T., Canil, D., & Heaman, L. (2007). Permian exhumation of the Buffalo Pitts orogenic peridotite massif, northern Cordillera, Yukon. *Canadian Journal of Earth Sciences*, *44*(3), 275–286. https://doi.org/10.1139/E06-078

Johnston, S. T., & Erdmer, P. (1995). Hot-side-up aureole in southwest Yukon and limits on terrane assembly of the northern Canadian Cordillera. *Geology*, *23*(5), 419–422. https://doi.org/10.1130/0091-7613(1995)023<0419:hsuais>2.3.co;2

Johnston, S. T., Mortensen, J. K., & Erdmer, P. (1996). Igneous and metaigneous age constraints for the Aishihik metamorphic suite, southwest Yukon. *Canadian Journal of Earth Sciences*, *33*(11), 1543–1555. https://doi.org/10.1139/e96-117

Jones, D. L., Howell, D. G., Coney, P. J., & Monger, J. W. H. (1983). Recognition, character and analysis of tectono-stratigraphic terranes in western North America. In M. Hashimoto & S. Uyeda (Eds.), *Accretion Tectonics in the Circum-Pacific Region* (pp. 21–35). Terra.

Kovacs, N., Allan, M. M., Crowley, J. L., Colpron, M., Hart, C. J. R., Zagorevski, A., & Creaser, R. A. (2020). Carmacks Copper Cu-Au-Ag deposit: Mineralization and post-ore migmatization of a Stikine arc porphyry copper system in Yukon, Canada. *Economic Geology*, *115*(7), 1413–1442. https://doi.org/10.5382/econgeo.4756

Kretz, R. (1983). Symbols for rock-forming minerals. *American Mineralogist*, *68*, 277–279.

Kroeger, E. D. L., McClelland, W. C., Colpron, M., Piercey, S. J., & Gehrels, G. E. (2023). Detrital zircon U-Pb and Hf isotope signature of Carboniferous and older strata of the Yukon-Tanana terrane in Yukon, Canadian Cordillera: Implications for terrane correlations and the onset of Late Devonian arc magmatism. *Geosphere*, *19*(4), 1032–1056. https://doi.org/10.1130/GES02607.1

Lapierre, H., Bosch, D., Tardy, M., & Struik, L. C. (2003). Late Paleozoic and Triassic plume-derived magmas in the Canadian Cordillera played a key role in continental growth. *Chemical Geology*, *201*(1–2), 55–89. https://doi.org/10.1016/s0009-2541(03)00224-9

Lawton, T. F., Cashman, P. H., Trexler, J. H., Jr., & Taylor, W. J. (2017). The late Paleozoic Southwestern Laurentian Borderland. *Geology*, *45*, 675–678.

Linde, G. M., Trexler, J. H., Jr., Cashman, P. H., Gehrels, G. E., & Dickinson, W. R. (2016). Detrital zircon U-Pb geochronology and Hf isotope geochemistry of the Roberts Mountains allochthon: New insights into the early Paleozoic tectonics of western North America. *Geosphere*, *12*(3), 1016–1031. https://doi.org/10.1130/ges01252.1

Liverton, T., Mortensen, J. K., & Roots, C. F. (2005). Character and metallogeny of Permian, Jurassic and Cretaceous plutons in the southern Yukon-Tanana terrane. In D. S. Emond, L. L. Lewis, & G. D. Bradshaw (Eds.), *Yukon Exploration and Geology 2004* (pp. 147–165). Yukon Geological Survey.

Ludwig, K. R. (2008). *Isoplot 3.70 - A geochronological toolkit for Microsoft Excel*. Berkeley Geochronology Center.

Ludwig, K. R., & Mundil, R. (2002). Extracting reliable U-Pb ages and errors from complex populations of zircons from Phanerozoic tuffs. *Geochimica et Cosmochimica Acta*, *66*(Supplement 1), A463.

MacKenzie, D., & Craw, D. (2012). Contrasting structural settings of mafic and ultramafic rocks in the Yukon-Tanana terrane. In K. E. MacFarlane & P. J. Sack (Eds.), *Yukon Exploration and Geology 2011* (pp. 115–127). Yukon Geological Survey.

MacKenzie, D., Craw, D., & Mortensen, J. K. (2008a). Thrust slices and associated deformation in the Klondike goldfields, Yukon. In D. S. Emond, L. R. Blackburn, R. P. Hill, & L. H. Weston (Eds.), *Yukon Exploration and Geology 2007* (pp. 199–213). Yukon Geological Survey.

MacKenzie, D., Craw, D., Mortensen, J. K., & Liverton, T. (2007). Structure of schist in the vicinity of the Klondike goldfield, Yukon. In D. S. Emond, L. L. Lewis, & L. H. Weston (Eds.), *Yukon Exploration and Geology 2006* (pp. 197–212). Yukon Geological Survey.

MacKenzie, D. J., Craw, D., & Mortensen, J. K. (2008b). Structural controls on orogenic gold mineralization in the Klondike goldfield, Canada. *Mineralium Deposita*, *43*(4), 435–448. https://doi.org/10.1007/s00126-007-0173-z

Manor, M. J., Piercey, S. J., Murphy, D. C., & Wall, C. J. (2022). Age and chemostratigraphy of the Finlayson Lake district, Yukon: Implications for volcanogenic massive sulfide (VMS) mineralization and tectonics along the western Laurentian continental margin. *Lithosphere*, *2022*(1), 45. https://doi.org/10.2113/2022/4584611

McClelland, W. C., Gilotti, J. A., Ramarao, T., Stemmerik, L., & Dalhoff, F. (2016). Carboniferous basin in Holm Land records local exhumation of the North-East Greenland Caledonides: Implications for the detrital zircon signature of a collisional orogen. *Geosphere*, *12*(3), 925–947. https://doi.org/10.1130/GES01284.1

McClelland, W. C., Strauss, J. V., Colpron, M., Gilotti, J. A., Faehnrich, K., Malone, S. J., et al. (2021). Taters versus Sliders: Evidence for a long-lived history of strike-slip displacement along the Canadian Arctic Transform Systems (CATS). *GSA Today*, *31*(7), 4–11. https://doi.org/10.1130/GSATG500A.1

McClelland, W. C., Strauss, J. V., Gilotti, J. A., & Colpron, M. (2022). Paleozoic evolution of the northern Laurentian margin: Evaluating links between Caledonian, Ellesmerian and Cordilleran orogens. In S. J. Whitmeyer, M. L. Williams, D. A. Kellett, & B. Tikoff (Eds.), *Laurentia: Turning points in the evolution of a continent*, *Memoir* (Vol. 220, pp. 605–633). Geological Society of America.

Mihalynuk, M. G., Mountjoy, K. J., Smith, M. T., Currie, L. D., Gabites, J. E., Tipper, H. W., et al. (1999). *Geology and mineral resources of the Tagish Lake area (NTS 104M/8, 9, 10E, 15 and 104N/12W), northwestern British Columbia* (Bulletin 105). B.C. Ministry of Energy and Mines.

Mihalynuk, M. G., Nelson, J., & Diakow, L. J. (1994). Cache Creek terrane entrapment: Oroclinal paradox within the Canadian Cordillera. *Tectonics*, *13*(3), 575–595. https://doi.org/10.1029/93tc03492

Miller, E. L., Kuznetsov, N., Soboleva, A., Udoratina, O., Grove, M. J., & Gehrels, G. E. (2011). Baltica in the Cordillera? *Geology*, *39*(8), 791–794. https://doi.org/10.1130/g31910.1

Miller, E. L., Miller, M. M., Stevens, C. H., Wright, J. E., & Madrid, R. (1992). Late Paleozoic paleogeographic and tectonic evolution of the western U.S. Cordillera. In B. C. Burchfiel, P. W. Lipman, & M. L. Zoback (Eds.), *The Cordilleran Orogen: Conterminous U.S.*, *The Geology of North America* (Vol. G-3, pp. 57–106). Geological Society of America. https://doi.org/10.1130/dnag-gna-g3.57

Monger, J. W. H., & Gibson, H. D. (2019). Mesozoic-Cenozoic deformation in the Canadian Cordillera: The record of a "Continental Bulldozer". *Tectonophysics*, *757*, 153–169. https://doi.org/10.1016/j.tecto.2018.12.023

Monger, J. W. H., & Nokleberg, W. J. (1996). Evolution of the northern North American Cordillera: Generation, fragmentation, displacement and accretion of successive North American plate-margin arcs. In A. R. Coyner & P. L. Fahey (Eds.), *Geology and Ore Deposits of the American Cordillera*, *Symposium Proceedings* (Vol. 3, pp. 1133–1152). Geological Society of Nevada.

Monger, J. W. H., Souther, J. G., & Gabrielse, H. (1972). Evolution of the Canadian Cordillera: A plate-tectonic model. *American Journal of Science*, *272*(7), 577–602. https://doi.org/10.2475/ajs.272.7.577

Monger, J. W. H., Wheeler, J. O., Tipper, H. W., Gabrielse, H., Harms, T., Struik, L. C., et al. (1991). Part B. Cordilleran terranes, Upper Devonian to Middle Jurassic assemblages (Chapter 8). In H. Gabrielse & C. J. Yorath (Eds.), *Geology of the Cordilleran orogen in Canada* (Vol. 4, pp. 281–327). Geological Survey of Canada.

Mortensen, J. K. (1988a). *Geology of southwestern Dawson map area (NTS 116 B. C)* (Open File 1927). Geological Survey of Canada.

Mortensen, J. K. (1988b). Geology of southwestern Dawson map area, Yukon Territory (NTS 116 B, C). In *Current Research, Part E*, *Paper 88-1E* (pp. 73–78). Geological Survey of Canada.

Mortensen, J. K. (1990). Geology and U-Pb geochronology of the Klondike District, west-central Yukon. *Canadian Journal of Earth Sciences*, *27*(7), 903–914. https://doi.org/10.1139/e90-093

Mortensen, J. K. (1992). Pre-Mid-Mesozoic tectonic evolution of the Yukon-Tanana terrane, Yukon and Alaska. *Tectonics*, *11*(4), 836–853. https://doi.org/10.1029/91tc01169

Mortensen, J. K. (1996). *Geological compilation maps of the northern Stewart River map area, Klondike and Sixtymile districts (115 N/15,16; 115 O/13,14 and parts of 115 O/15,16)*. (Open File 1996-1(G)). Yukon Geological Survey.

Mortensen, J. K., Erdmer, P., & Ghent, E. D. (1997). Westerly-derived Upper Triassic clastic sedimentary rocks in southeastern Yukon: Evidence for early Mesozoic terrane interaction with the western margin of Ancestral North America. In F. Cook & P. Erdmer (Eds.), *Slave–Northern Cordillera Lithospheric Transect and Cordilleran Tectonics Workshop*, *Lithoprobe Report* (Vol. 56, p. 76). University of Calgary. Retrieved from https://data.geology.gov.yk.ca/Reference/96084

Moynihan, D. P., & Crowley, J. L. (2022). Preliminary observations on the geology of the southern Big Salmon Range, south-central Yukon (parts of NTS 105C/13, 14, 105F/4 and 105E/1). In K. E. MacFarlane (Ed.), *Yukon Exploration and Geology 2021* (pp. 217–265). Yukon Geological Survey.

Murphy, D. C., Mortensen, J. K., Piercey, S. J., Orchard, M. J., & Gehrels, G. E. (2006). Mid-Paleozoic to early Mesozoic tectonostratigraphic evolution of Yukon-Tanana and Slide Mountain terranes and affiliated overlap assemblages, Finlayson Lake massive sulphide district, southeastern Yukon. In M. Colpron & J. L. Nelson (Eds.), *Paleozoic Evolution and Metallogeny of Pericratonic Terranes at the Ancient Pacific Margin of North America, Canadian and Alaskan Cordillera*, *Special Paper* (Vol. 45, pp. 75–105). Geological Association of Canada.

Nelson, J. L. (1993). The Sylvester allochthon: Upper Paleozoic marginal-basin and island-arc terranes in northern British Columbia. *Canadian Journal of Earth Sciences*, *30*(3), 631–643. https://doi.org/10.1139/e93-048

Nelson, J. L., Colpron, M., & Israel, S. (2013). The Cordillera of British Columbia, Yukon, and Alaska: Tectonics and metallogeny. In M. Colpron, T. Bissig, B. G. Rusk, & J. F. H. Thompson (Eds.), *Tectonics, Metallogeny and Discovery: The North American Cordillera and Similar Accretionary Settings*, *Special Publication* (Vol. 17, pp. 53–103). Society of Economic Geologists, Inc.

Nelson, J. L., Colpron, M., Piercey, S. J., Dusel-Bacon, C., Murphy, D. C., & Roots, C. F. (2006). Paleozoic tectonic and metallogenic evolution of the pericratonic terranes in Yukon, northern British Columbia and eastern Alaska. In M. Colpron & J. L. Nelson (Eds.), *Paleozoic Evolution and Metallogeny of Pericratonic Terranes at the Ancient Pacific Margin of North America, Canadian and Alaskan Cordillera*, *Special Paper* (Vol. 45, pp. 323–360). Geological Association of Canada.

Nelson, J. L., & Friedman, R. M. (2004). Superimposed Quesnel (late Paleozoic-Jurassic) and Yukon-Tanana (Devonian-Mississippian) arc assemblages, Cassiar Mountains, northern British Columbia: Field, U-Pb and igneous petrochemical evidence. *Canadian Journal of Earth Sciences*, *41*(10), 1201–1235. https://doi.org/10.1139/e04-028

Nelson, J. L., van Straaten, B., & Friedman, R. (2022). Latest Triassic-Early Jurassic Stikine – Yukon-Tanana terrane collision and the onset of accretion in the Canadian Cordillera: Insights from Hazelton Group detrital zircon provenance and arc–back-arc configuration. *Geosphere*, *18*(2), 670–696. https://doi.org/10.1130/GES02444.1

Nixon, G. T., Scheel, J. E., Scoates, J. S., Friedman, R. M., Wall, C. J., Gabites, J., & Jackson-Brown, S. (2020). Syn-accretionary multistage assembly of an Early Jurassic Alaskan-type intrusion in the Canadian Cordillera: U-Pb and $^{40}Ar/^{39}Ar$ geochronology of the Turnagain ultramafic-mafic intrusive complex, Yukon-Tanana terrane. *Canadian Journal of Earth Sciences*, *57*(5), 575–600. https://doi.org/10.1139/cjes-2019-0121

Nokleberg, W. J., Parfenov, L. M., Monger, J. W. H., Norton, I. O., Khanchuk, A. I., Stone, D. B., et al. (2000). *Phanerozoic tectonic evolution of the circum-North Pacific* (Professional Paper 1626). U.S. Geological Survey.

Ootes, L., Milidragovic, D., Friedman, R., Wall, C., Cordey, F., Luo, Y., et al. (2022). A juvenile Paleozoic ocean floor origin for eastern Stikinia, Canadian Cordillera. *Geosphere*, *18*(4), 1297–1315. https://doi.org/10.1130/GES02459.1

Orchard, M. J. (2006). Late Paleozoic and Triassic conodont faunas of Yukon Territory and northern British Columbia and implications for the evolution of the Yukon-Tanana terrane. In M. Colpron & J. L. Nelson (Eds.), *Paleozoic Evolution and Metallogeny of Pericratonic Terranes at the Ancient Pacific Margin of North America, Canadian and Alaskan Cordillera*, *Special Paper* (Vol. 45, pp. 229–260). Geological Association of Canada.

Pană, D. I., Poulton, T. P., & DuFrane, S. A. (2018). U-Pb detrital zircon dating supports Early Jurassic initiation of the Cordilleran foreland basin in southwestern Canada. *Geological Society of America Bulletin*, *131*(1–2), 318–334. https://doi.org/10.1130/b31862.1

Parsons, A. J., Zagorevski, A., Ryan, J. J., McClelland, W. C., van Staal, C. R., Coleman, M. J., & Golding, M. L. (2019). Petrogenesis of the Dunite Peak ophiolite, south-central Yukon, and the distinction between upper-plate and lowerplate settings: A new hypothesis for the late Paleozoic–early Mesozoic tectonic evolution of the Northern Cordillera. *Geological Society of America Bulletin*, *131*(1–2), 274–298. https://doi.org/10.1130/b31964.1

Pearce, J. A. (1996). A user's guide to basalt discrimination diagrams. In D. A. Wyman (Ed.), *Trace element geochemistry of volcanic rocks: Applications for massive sulphide exploration*, *Short Course Notes* (Vol. 12, pp. 79–113). Geological Association of Canada.

Pearce, J. A. (2014). Immobile element fingerprinting of ophiolites. *Elements*, *10*(2), 101–108. https://doi.org/10.2113/gselements.10.2.101

Pearce, J. A., Harris, N. B. W., & Tindle, A. G. (1984). Trace element discrimination diagrams for the tectonic interpretation of granitic rocks. *Journal of Petrology*, *25*(4), 956–983. https://doi.org/10.1093/petrology/25.4.956

Pearce, J. A., & Peate, D. W. (1995). Tectonic implications of the composition of volcanic arc magmas. *Annual Reviews of Earth and Planetary Science*, *23*(1), 251–285. https://doi.org/10.1146/annurev.ea.23.050195.001343

Pearce, J. A., & Stern, R. J. (2006). Origin of back-arc basin magmas: Trace element and isotope perspectives. In *Back-Arc Spreading Systems: Geological, Biological, Chemical, and Physical Interactions*, *Geophysical Monograph Series* (Vol. 166, pp. 63–86). American Geophysical Union. https://doi.org/10.1029/166gm06

Pecha, M. E., Gehrels, G. E., McClelland, W. C., Giesler, D., White, C., & Yokelson, I. (2016). Detrital zircon U-Pb geochronology and Hf isotope geochemistry of the Yukon-Tanana terrane, Coast Mountains, southeast Alaska. *Geosphere*, *12*(5), 1556–1574. https://doi.org/10.1130/ges01303.1

Perchuk, A., & Philippot, P. (2000). Nascent subduction: A record in the Yukon eclogites. *Petrology*, *1*, 3–22.

Petrie, M. B., Gilotti, J. A., McClelland, W. C., van Staal, C. R., & Isard, S. J. (2015). Geologic setting of eclogite-facies assemblages in the St. Cyr klippe, Yukon-Tanana terrane, Yukon, Canada. *Geoscience Canada*, *42*(3), 327–350. https://doi.org/10.12789/geocanj.2015.42.073

Petrie, M. B., Massonne, H.-J., Gilotti, J. A., McClelland, W. C., & van Staal, C. R. (2016). The *P-T* path of eclogite in the St. Cyr klippe, Yukon, Canada: Permian metamorphism of a coherent high-pressure unit in an accreted terrane of the North American Cordillera. *European Journal of Mineralogy*, *28*(6), 1111–1130. https://doi.org/10.1127/ejm/2016/0028-2576

Philippot, P., Blichert-Toft, J., Perchuk, A., Costa, S., & Gerasimov, V. (2001). Lu-Hf and Ar-Ar chronometry supports extreme rate of subduction zone metamorphism deduced from geospeedometry. *Tectonophysics*, *342*(1–2), 23–38. https://doi.org/10.1016/S0040-1951(01)00155-X

Piercey, S. J., & Colpron, M. (2009). Composition and provenance of the Snowcap assemblage, basement to the Yukon-Tanana terrane, northern Cordillera: Implications for Cordilleran crustal growth. *Geosphere*, *5*, 439–464. https://doi.org/10.1130/GES00505.1

Piercey, S. J., Murphy, D. C., & Creaser, R. A. (2012). Lithosphere-asthenosphere mixing in a transform-dominated late Paleozoic barc-arc basin: Implications for northern Cordilleran crustal growth and assembly. *Geosphere*, *8*(3), 716–739. https://doi.org/10.1130/ges00757.1

Piercey, S. J., Nelson, J. L., Colpron, M., Dusel-Bacon, C., Roots, C. F., & Simard, R.-L. (2006). Paleozoic magmatism and crustal recycling along the ancient Pacific margin of North America, northern Cordillera. In M. Colpron & J. L. Nelson (Eds.), *Paleozoic Evolution and Metallogeny of Pericratonic Terranes at the Ancient Pacific Margin of North America, Canadian and Alaskan Cordillera*, *Special Paper* (Vol. 45, pp. 281–322). Geological Association of Canada.

Pigage, L. C. (2004). *Bedrock geology compilation of the Anvil District (parts of 105K/2, 3, 5, 6, 7 and 11), central Yukon* (Bulletin 15). Yukon Geological Survey.

Powerman, V., Hanson, R., Nosova, A., Girty, G. H., Hourigan, J., & Tretiakov, A. (2020). Nature and timing of Late Devonian–early Mississippian island-arc magmatism in the Northern Sierra terrane and implications for regional Paleozoic plate tectonics. *Geosphere*, *16*(1), 258–280. https://doi.org/10.1130/GES02105.1

Read, P. B., Woodsworth, G. J., Greenwood, H. J., Ghent, E. D., & Evenchick, C. A. (1991). *Metamorphic map of the Canadian Cordillera (Map 1714A)*. Geological Survey of Canada.

Richards, D. R., Butler, R. F., & Harms, T. A. (1993). Paleomagnetism of the late Paleozoic Slide Mountain terrane, northern and central British Columbia. *Canadian Journal of Earth Sciences*, *30*(9), 1898–1913. https://doi.org/10.1139/e93-168

Roddick, J. A. (1967). Tintina Trench. *Journal of Geology*, *75*(1), 23–33. https://doi.org/10.1086/627228

Roots, C. F., Nelson, J. L., Simard, R.-L., & Harms, T. A. (2006). Continental fragments, mid-Paleozoic arcs and overlapping late Paleozoic arc and Triassic sedimentary strata in the Yukon-Tanana terrane of northern British Columbia and southern Yukon. In M. Colpron & J. L. Nelson (Eds.), *Paleozoic Evolution and Metallogeny of Pericratonic Terranes at the Ancient Pacific Margin of North America, Canadian and Alaskan Cordillera*, *Special Paper* (Vol. 45, pp. 153–177). Geological Association of Canada.

Ruks, T. W., Piercey, S. J., Ryan, J. J., Villeneuve, M. E., & Creaser, R. A. (2006). Mid- to late Paleozoic K-feldspar augen granitoids of the Yukon-Tanana terrane, Yukon, Canada: Implications for crustal growth and tectonic evolution of the northern Cordillera. *Geological Society of America Bulletin*, *118*(9–10), 1212–1231. https://doi.org/10.1130/B25854.1

Ryan, J. J., Zagorevski, A., Cleven, N. R., Parsons, A. J., & Joyce, N. L. (2021). Architecture of pericratonic Yukon-Tanana terrane in the northern Cordillera. In J. J. Ryan & A. Zagorevski (Eds.), *Northern Cordillera geology: A synthesis of research from the Geo-mapping for Energy and Minerals program, British Columbia and Yukon*, *Bulletin* (Vol. 610, pp. 67–93). Geological Survey of Canada.

Shervais, J. W. (2022). The petrogenesis of modern and ophiolitic lavas reconsidered: Ti-V and Nb-Th. *Geoscience Frontiers*, *13*(2), 101319. https://doi.org/10.1016/j.gsf.2021.101319

Snyder, W. S., Brueckner, H. K., & Northrup, C. J. (2022). Sonoma orogeny – A reassessment. In *Late Paleozoic and early Mesozoic tectonostratigraphy and biostratigraphy of western Pangea*. In *Special Publication* (Vol. 113, pp. 172–204). Society for Sedimentary Geology (SEPM). https://doi.org/10.2110/sepmsp.113.11

Soja, C. M. (2008). Silurian-bearing terranes of Alaska. In R. B. Blodgett & G. D. StanleyJr (Eds.), *The Terrane Puzzle: New Perspectives on Paleontology and Stratigraphy from the North American Cordillera*, *Special Paper* (Vol. 442, pp. 39–50). Geological Society of America. https://doi.org/10.1130/2008.442(02)

Soucy La Roche, R., Dyer, S. C., Zagorevski, A., Cottle, J. M., & Gaidies, F. (2022). 150 Myr of episodic metamorphism recorded in the Yukon-Tanana terrane, northern Canadian Cordillera: Evidence from monazite and xenotime petrochronology. *Lithosphere*, *2022*(1), 7708357. https://doi.org/10.2113/2022/7708357

Staples, R. D. (2014). *Diachronous deformation, metamorphism and exhumation in the northern Canadian Cordillera: Revealed from pressure-temperature-time-deformation paths of former mid-crustal rocks* (Ph.D. thesis). Simon Fraser University.

Staples, R. D., Gibson, H. D., Berman, R. G., Ryan, J. J., & Colpron, M. (2013). A window into the Early to mid-Cretaceous infrastructure of the Yukon-Tanana terrane recorded in multi-stage garnet of west-central Yukon, Canada. *Journal of Metamorphic Geology*, *31*(7), 729–753. https://doi.org/10.1111/jmg.12042

Staples, R. D., Gibson, H. D., Colpron, M., & Ryan, J. J. (2016). An orogenic wedge model for diachronous deformation, metamorphism, and exhumation in the hinterland of the northern Canadian Cordillera. *Lithosphere*, *8*(2), 165–184. https://doi.org/10.1130/L472.1

Staples, R. D., Murphy, D. C., Gibson, H. D., Colpron, M., Berman, R. G., & Ryan, J. J. (2014). Middle Jurassic to earliest Cretaceous mid-crustal tectono-metamorphism in the northern Canadian Cordillera: Recording foreland-directed migration of an orogenic front. *Geological Society of America Bulletin*, *126*(11–12), 1511–1530. https://doi.org/10.1130/b31037.1

Struik, L. C., & Orchard, M. J. (1985). Late Paleozoic conodonts from riddon chert delineate imbricate thrusts within the Antler Formation of the Slide Mountain terrane, central British Columbia. *Geology*, *13*(11), 794–798. https://doi.org/10.1130/0091-7613(1985)13%3C794:LPCFRC%3E2.0.CO;2

Sun, S. S., & McDonough, W. F. (1989). Chemical and isotopic systematics of oceanic basalts: Implications for mantle composition and processes. In A. D. Saunders & M. J. Norry (Eds.), *Magmatism in the ocean basins*, *Special Publication* (Vol. 42, pp. 313–345). Geological Society of London.

Sundell, K., Saylor, J. E., & Pecha, M. (2019). Provenance and recycling of detrital zircons from Cenozoic Altiplano strata and the crustal evolution of western South America from combined U-Pb and Lu-Hf isotopic analysis. In B. K. Horton & A. Folguera (Eds.), *Andean tectonics* (pp. 363–397). Elsevier Inc.

Sundell, K. E., Gehrels, G. E., & Pecha, M. E. (2021). Rapid U-Pb Geochronology by Laser Ablation Multi-Collector ICP-MS. *Geostandards and Geoanalytical Research*, *45*(1), 37–57. https://doi.org/10.1111/ggr.12355

Trexler, J. H., Jr., Cashman, P. H., Snyder, W. S., & Davydov, V. I. (2004). Late Paleozoic tectonism in Nevada: Timing, kinematics, and tectonic significance. *Geological Society of America Bulletin*, *116*(5), 525–538. https://doi.org/10.1130/b25295.1

van Drecht, L. H., Beranek, L. P., Colpron, M., & Wiest, A. C. (2022). Development of the Whitehorse trough as a strike-slip basin during Early to Middle Jurassic arc-continent collision in the Canadian Cordillera. *Geosphere*, *18*(5), 1538–1562. https://doi.org/10.1130/GES02510.1

van Staal, C. R., Zagorevski, A., McClelland, W. C., Escayola, M. P., Ryan, J. J., Parsons, A. J., & Proenza, J. (2018). Age and setting of Permian Slide Mountain terrane ophiolitic ultramafic-mafic complexes in the Yukon: Implications for late Paleozoic-early Mesozoic tectonic models in the northern Canadian Cordillera. *Tectonophysics*, *744*, 458–483. https://doi.org/10.1016/j.tecto.2018.07.008

Vervoort, J. D., Plank, T., & Prytulak, J. (2011). The Hf–Nd isotopic composition of marine sediments. *Geochimica et Cosmochimica Acta*, *75*(20), 5903–5926. https://doi.org/10.1016/j.gca.2011.07.046

Villeneuve, M. E., Ryan, J. J., Gordey, S. P., & Piercey, S. J. (2003). Detailed thermal and provenance history of the Stewart River area (Yukon-Tanana Terrane, western Yukon) through application of SHRIMP, Ar-Ar and TIMS. In *Joint Annual Meeting, Abstracts* (Vol. 28). Geological Association of Canada - Mineralogical Association of Canada - Society of Economic Geologists.

von Blanckenburg, F., & Davies, J. H. (1995). Slab breakoff: A model for syncollisional magmatism and tectonics in the Alps. *Tectonics*, *14*(1), 120–131. https://doi.org/10.1029/94tc02051

Wheeler, J. O., Brookfield, A. J., Gabrielse, H., Monger, J. W. H., Tipper, H. W., & Woodsworth, G. J. (1991). *Terrane map of the Canadian Cordillera (Map 1713A)*. Geological Survey of Canada.

Wilson, F. H., Hults, C. P., Mull, C. G., & Karl, S. M. (2015). *Geologic map of Alaska (Scientific Investigation Map 3340)*. U.S. Geological Survey.

Winchester, J. A., & Floyd, P. A. (1977). Geochemical discrimination of different magma series and their differentiation products using immobile elements. *Chemical Geology*, *20*, 325–343. https://doi.org/10.1016/0009-2541(77)90057-2

Yukon Geological Survey. (2023). *Yukon Geochronology – A database of Yukon isotopic age determinations*. Yukon Geological Survey. Retrieved from http://data.geology.gov.yk.ca/Compilation/22

Yukon Geological Survey. (2024). *Yukon Digital Bedrock Geology*. Yukon Geological Survey. Retrieved from http://datatest.geology.gov.yk.ca/Compilation/3

Zagorevski, A., & van Staal, C. R. (2021). Cordilleran magmatism in Yukon and northern British Columbia: Characteristics, temporal variations, and significance for the tectonic evolution of the northern Cordillera. In J. J. Ryan & A. Zagorevski (Eds.), *Northern Cordillera geology: A synthesis of research from the Geo-mapping for Energy and Minerals program, British Columbia and Yukon*, *Bulletin* (Vol. 610, pp. 95–122). Geological Survey of Canada.

Zagorevski, A., van Staal, C. R., Bédard, J. H., Bogatu, A., Canil, D., Coleman, M., et al. (2021). Overview of Cordilleran oceanic terranes and their significance for the tectonic evolution of the northern Cordillera. In J. J. Ryan & A. Zagorevski (Eds.), *Northern Cordillera geology: A synthesis of research from the Geo-mapping for Energy and Minerals program, British Columbia and Yukon*, *Bulletin* (Vol. 610, pp. 21–65). Geological Survey of Canada.